Cruise report 64PE358 on RV Pelagia

THOR-GEOTRACES western North Atlantic

Reykjavik (Iceland) 29-07-2012 to Texel (Netherlands) 19-08-2012

Micha J.A. Rijkenberg

With contributions of participants

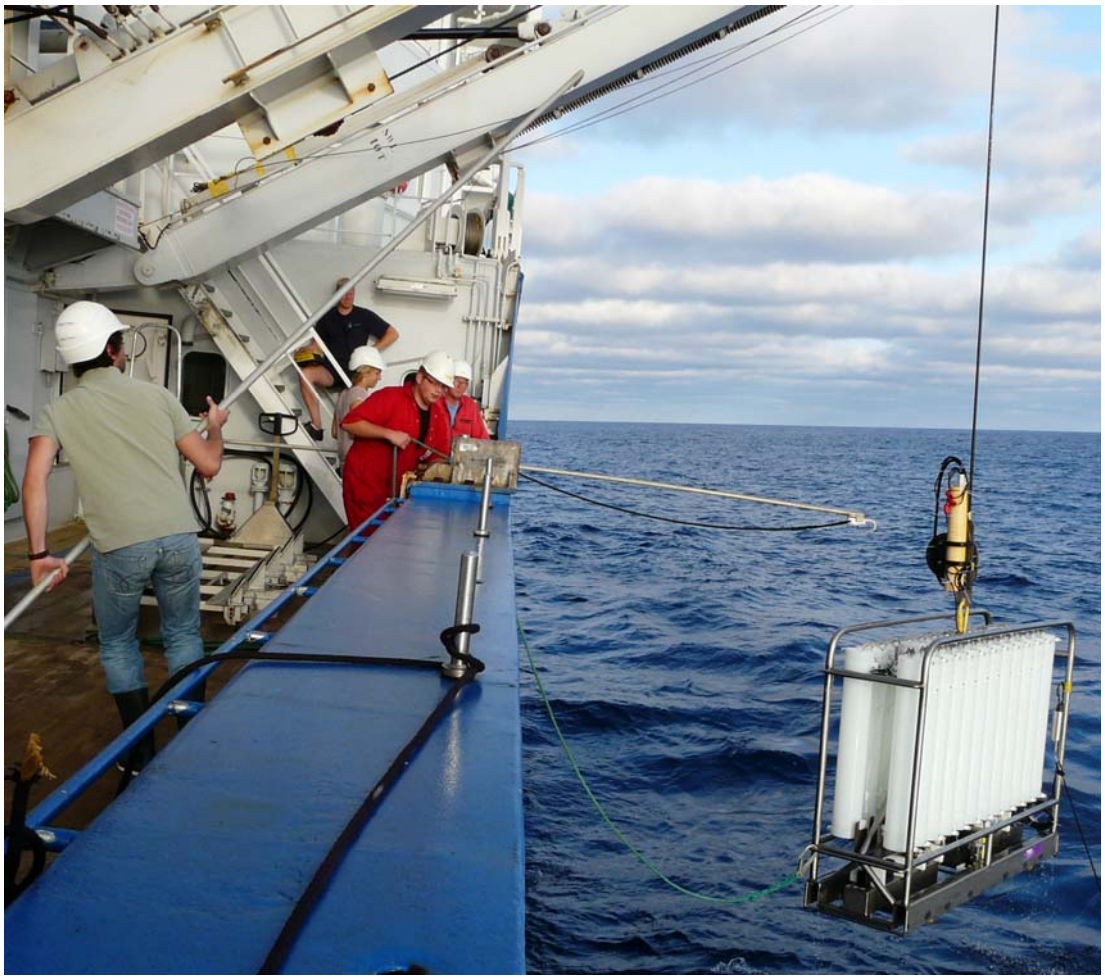

Royal Netherlands Institute for Sea Research

Acknowledgements

On behalf of all participants I want to thank Captain Pieter Kuijt for his help, advice and hospitality on his ship RV Pelagia. The crew of the Pelagia: Bert Puijman, Alle Fockema, Klaas Kikkert, Evgeny Vorobyev, Gert Vermeulen, Sjaak Maas, Freddy Hiemstra, Jacob Zwerver, Rik van Katwijk and Sergeys Nestrov were very helpful whenever and wherever needed. They made our stay on the Pelagia a convenient and happy time. The post-cruise data management by Hendrik van Aken and the data management group was excellent as usual. Other people I want to thank for their help to make this cruise possible are Hilde Kooijman (NIOZ), Erica Koning (NIOZ), Jack Schilling (NIOZ) and everybody from the NIOZ MTEC department involved in getting all our equipment organised! We acknowledge Royal NIOZ for financing of the ship time and part of the cruise support.

Front page: the titanium ultraclean CTD frame with 24 x 27L PVDF samplers during recovery on the RV Pelagia

CONTENTS

Cruise summary

Research cruise

The THOR-GEOTRACES western North Atlantic GEOTRACES cruise 64PE358 on RV Pelagia started 29 July 2012 departing from Reykjavik (Iceland) and ended in the NIOZ harbour on Texel (The Netherlands) on 20 August 2012 with Micha Rijkenberg (Royal NIOZ) as chief scientist.

Stations

During cruise 64PE358 we occupied a total of 14 stations (Figure 1). The first station was a test station to 100 m depth to check the sensors of the ultraclean CTD (UCC). The second station was the LOCO2 mooring site at 59°12.35'N and 39°30.53'W. Here a mooring belonging to the Physical Oceanography department at NIOZ was serviced (project: THOR, PI: Laura de Steur). To investigate the physical oceanographic setting before and after servicing of the mooring at LOCO2 two casts (cast 3 & 5) were executed with the UCC. Stations 3-7 were executed to complete the western North Atlantic GEOTRACES transect as sampled during Netherlands GEOTRACES leg 1 (64PE319) (Figure 2). During 64PE319, storms made it impossible to sample these stations. A full depth and a shallow cast were performed at each of the stations 3-7. The deep casts were executed as part of GEOTRACES and the shallow casts were executed as part of a GEOTRACES process study to investigate the internal cycling of Fe, Co, Zn and Cd in the upper 300 m of the water column. Their distribution was determined with respect to their dissolved, colloidal and truly soluble fraction as well as their organic complexation (Fe and Co) in relation to phytoplankton abundance and the physical oceanography in the upper 280 m of the water column. Seven extra shallow stations 8-14 were performed on our transect back to Texel. These shallow stations extended the dataset for the fine distribution of Fe, Co, Zn and Cd (stations 8-12), extended the dataset that investigates the photo-acclimation of phytoplankton (stations 8-14), and investigated the CO_2 system along the Warm Gulf Stream and beyond (stations 8–14).

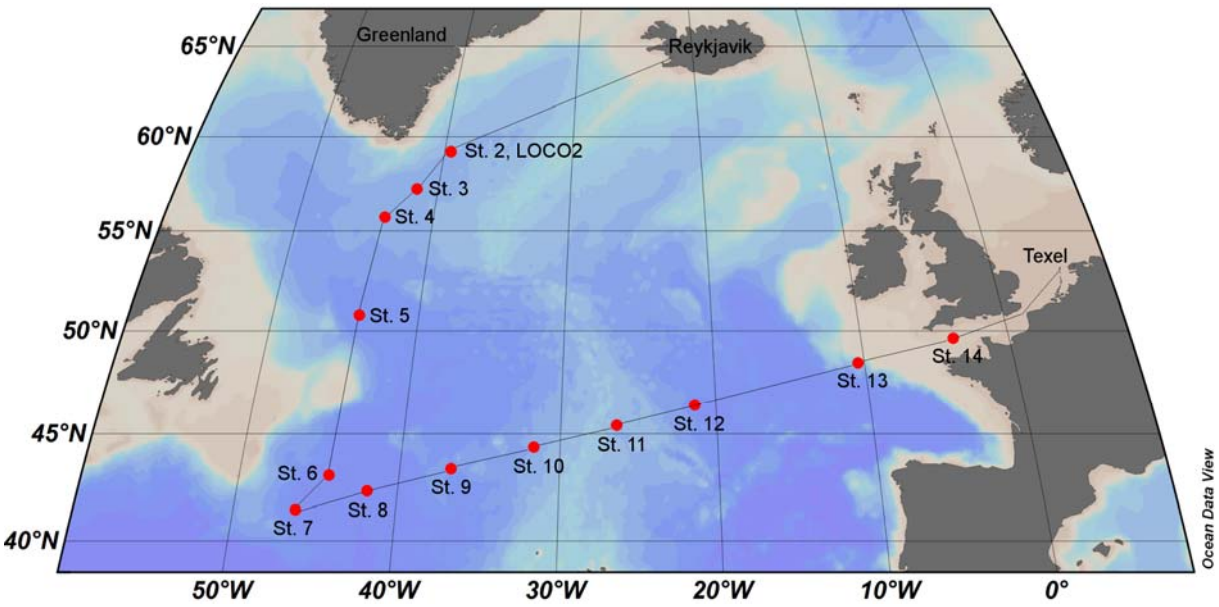

Figure 1. Cruise track of research cruise 64PE358 on the RV Pelagia in July-August 2012.

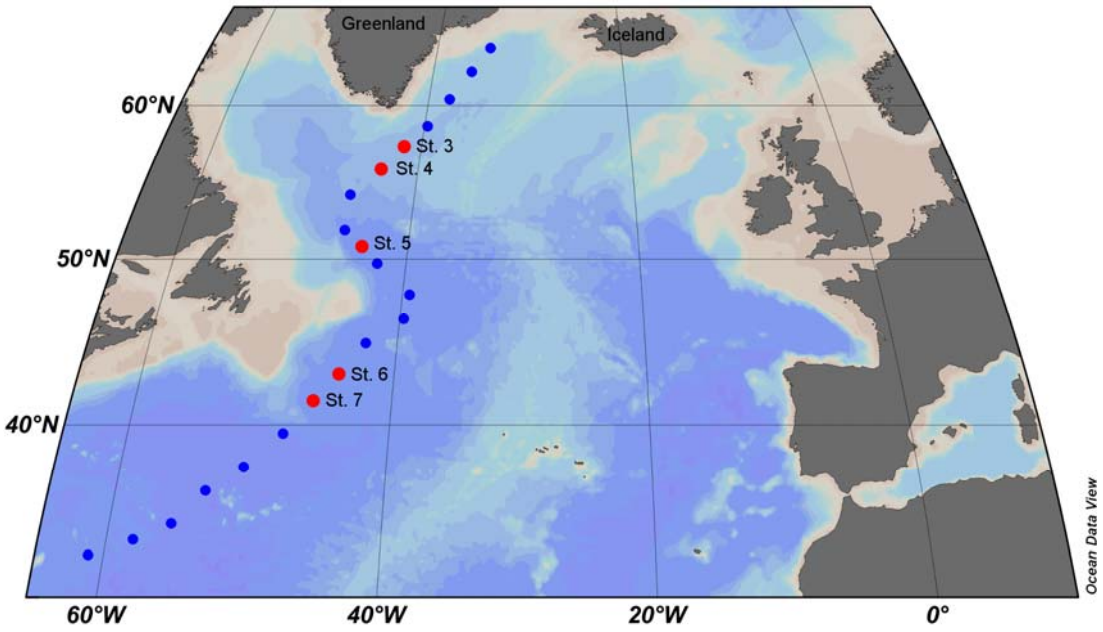

Figure 2. The stations 3-7 of cruise 64PE358 (red dots) in context to the stations sampled during the first GEOTRACES leg, cruise 64PE319 (blue dots).

Cruise narrative

The participants boarded the RV Pelagia on 29 July in Reykjavik, Iceland. We left Reykjavik with calm weather. We arrived at the LOCO2 mooring site on 1 August. The successful recovery of the mooring, extracting of the data and redeployment of the mooring took 2 days.

Before sampling of the GEOTRACES stations we tested the PVDF bottles of the ultraclean CTD for Fe contamination. No Fe contamination was observed. We arrived at the first GEOTRACES station (st. 3) in the morning of 3 August. All following GEOTRACES stations 4-7 were also sampled under excellent weather conditions. Due to the excellent weather conditions we were able to sample another 7 shallow stations (280 m) for trace metals (dissolved and 0.02 µm size fractionated), nutrients and the CO_2 system on our way back to Texel. In addition to 7 shallow stations, we filled 3 cubic meter vessels with unfiltered nutrient poor seawater for Corina Brussaard (Royal NIOZ), Table 1. We also filled 2 cubic meter vessels with trace metal clean 0.2 µm filtered surface seawater for Patrick Laan (Royal NIOZ). One station planned for sampling nutrients, the CO_2 system and phytoplankton was cancelled on 15 August due to adverse weather conditions.

Table 1. Nutrient concentrations for the 3 cubic meter vessels as sampled on 11 August 2012 between 08:00-09:00 am at 43.34598 °N and -36.80296 °W for Corina Brussaard as measured by Sharyn Ossebaar.

	Phosphate (µmol/L)[1]	Silicate (µmol/L)[1]	Nitrate + Nitrite (µmol/L)[1]	Nitrite (µmol/L)
VAT PL01	0.014	0.399	0.018	0.011
VAT PL02	0.014	0.394	0.010	0.011
VAT PL15	0.017	0.399	0.005	0.014

[1] The detection limit for phosphate was 0.008 µmol/L, for silicate 0.012 µmol/L, nitrate + nitrite 0.013 µmol/L and for nitrite was 0.015 µmol/L.

Ship's clock

The ship left the harbour on 29 July 2012 with the ship's time set on UTC. The ship's time was advanced in the morning of 14 August 2012 to UTC+1hr and after arrival on 19 August to UTC+2hrs.

Weather

The weather conditions were excellent during most of the expedition. Wind speed did not exceed 20 m s^{-1}. Only one station planned for 15/08 needed to be cancelled due to adverse weather condition (Figure 3).

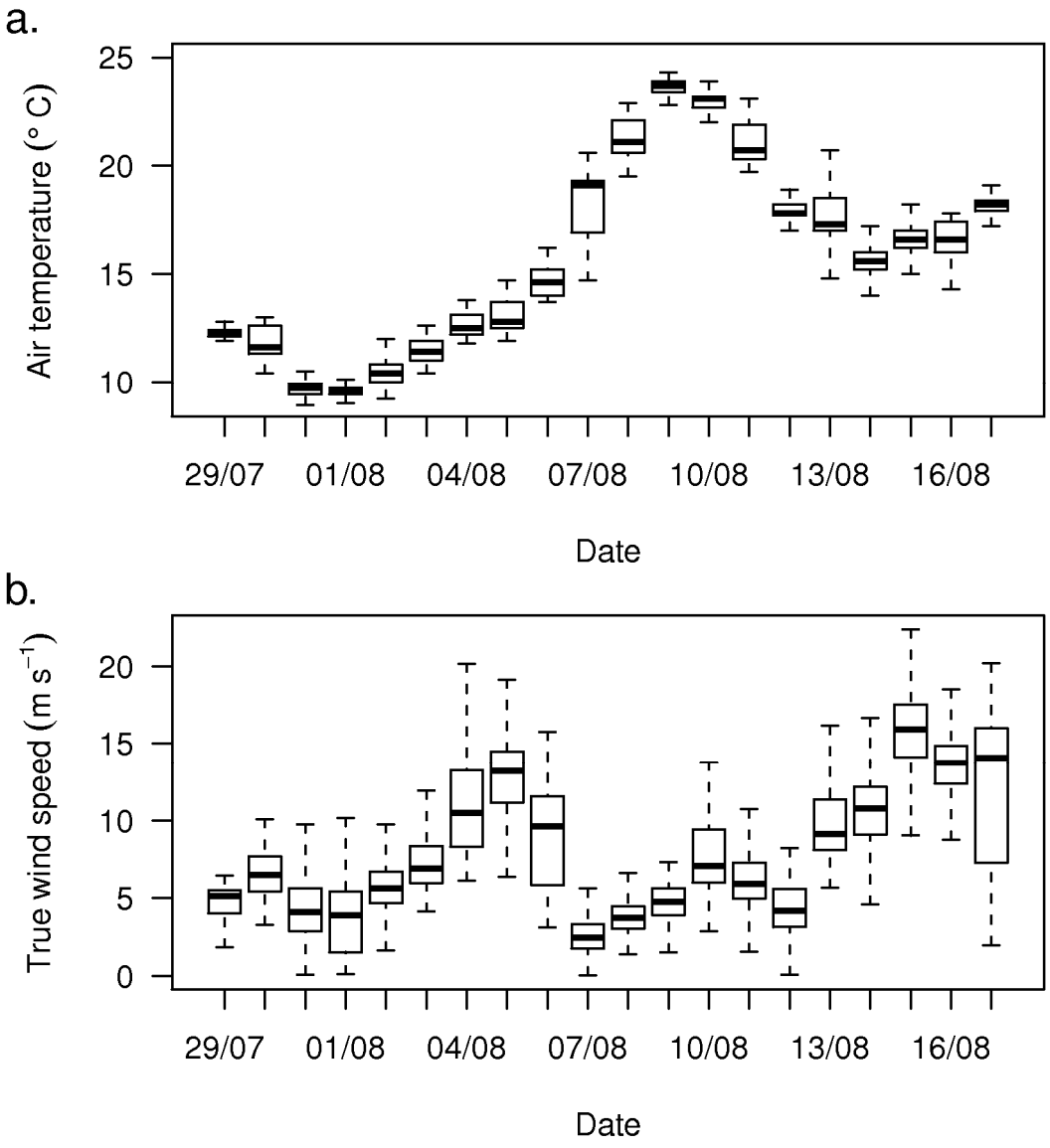

Figure 3. The air temperature (a.) and true wind speed (b.) during 64PE358.

General preliminary results

Parameters measured on board were the CTD sensor output (e.g. salinity, temperature, fluorescence, oxygen, beam attenuation coefficient) and the nutrients (phosphate, nitrate, nitrite and silicate). The salinity, phosphate, nitrate and silicate measured during 64PE358 fit

very well within the data of the transect sailed during GEOTRACES leg 1 (64PE319) (Figures 4, 5, 6, 7). The salinity at 1000m station 6 needs to be checked after calibration of the data. Clearly recognizable water masses were the Labrador Sea Water (LSW), North East Atlantic Deep Water (NEADW), Denmark Strait Overflow Water (DSOW), North Atlantic Deep Water (NADW) and the Antarctic Bottom Water (AABW).

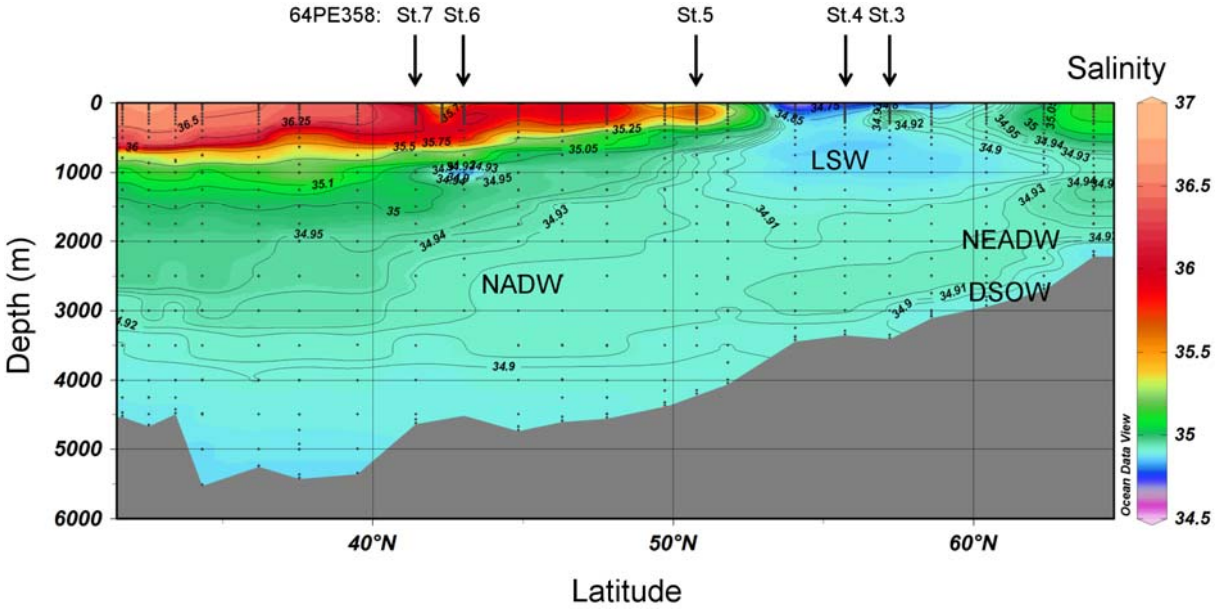

Figure 4. The full western North Atlantic GEOTRACES transect of salinity between Iceland and Bermuda with the stations visited during 64PE358 indicated. Data: Sven Ober.

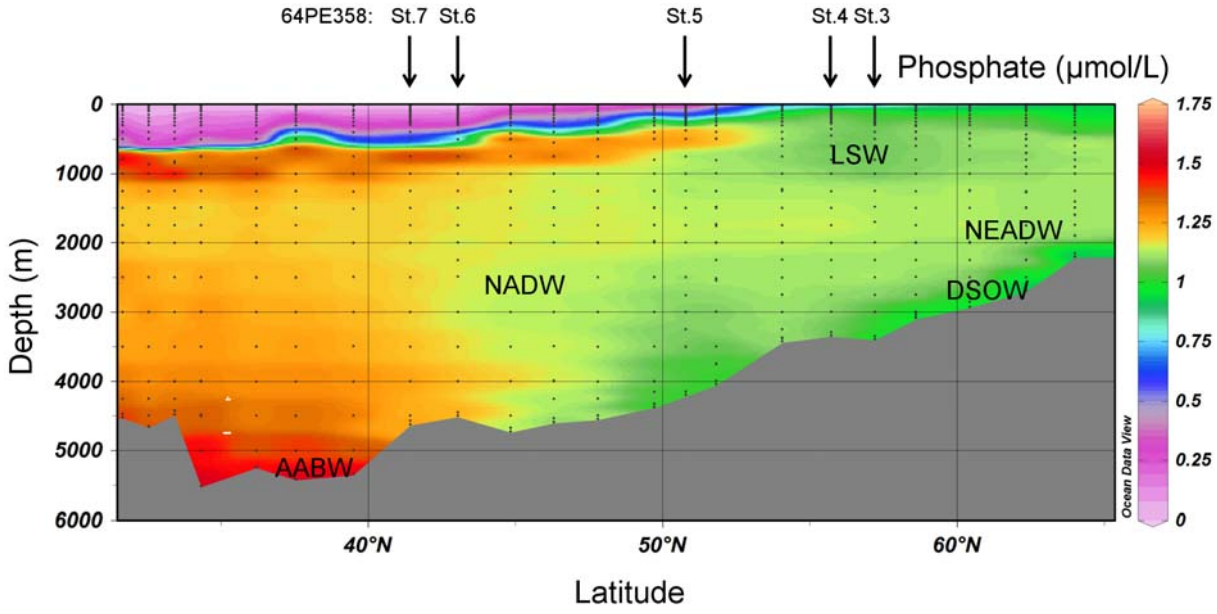

Figure 5. The full western North Atlantic GEOTRACES transect of phosphate between Iceland and Bermuda with the stations visited during 64PE358 indicated. Data: Sharyn Ossebaar.

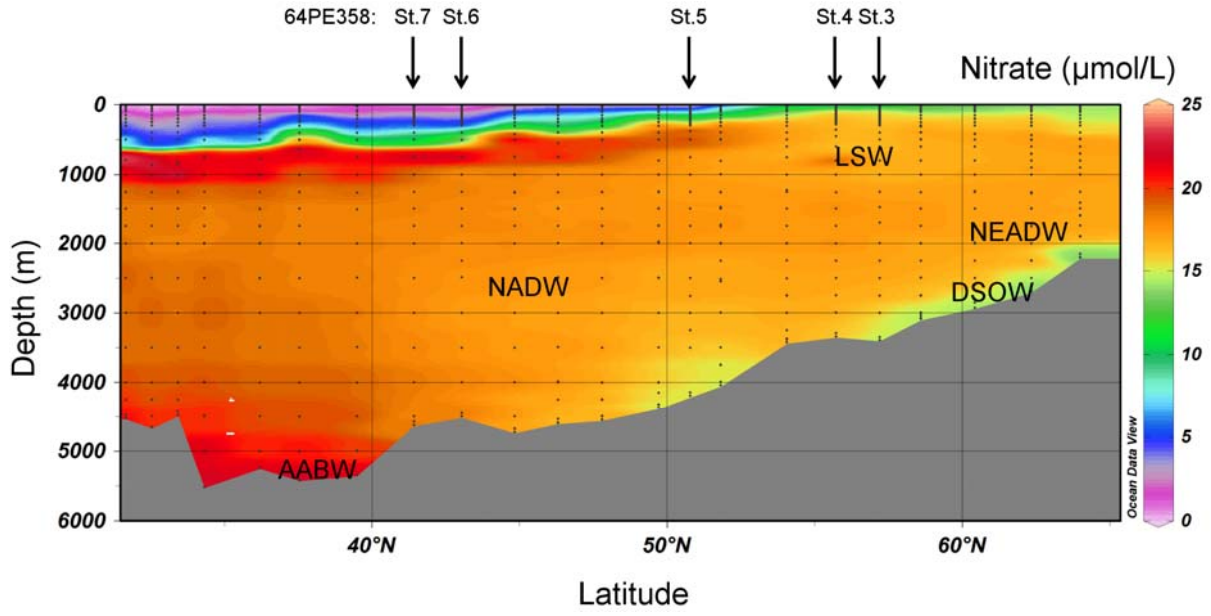

Figure 6. The full western North Atlantic GEOTRACES transect of nitrate between Iceland and Bermuda with the stations visited during 64PE358 indicated. Data: Sharyn Ossebaar.

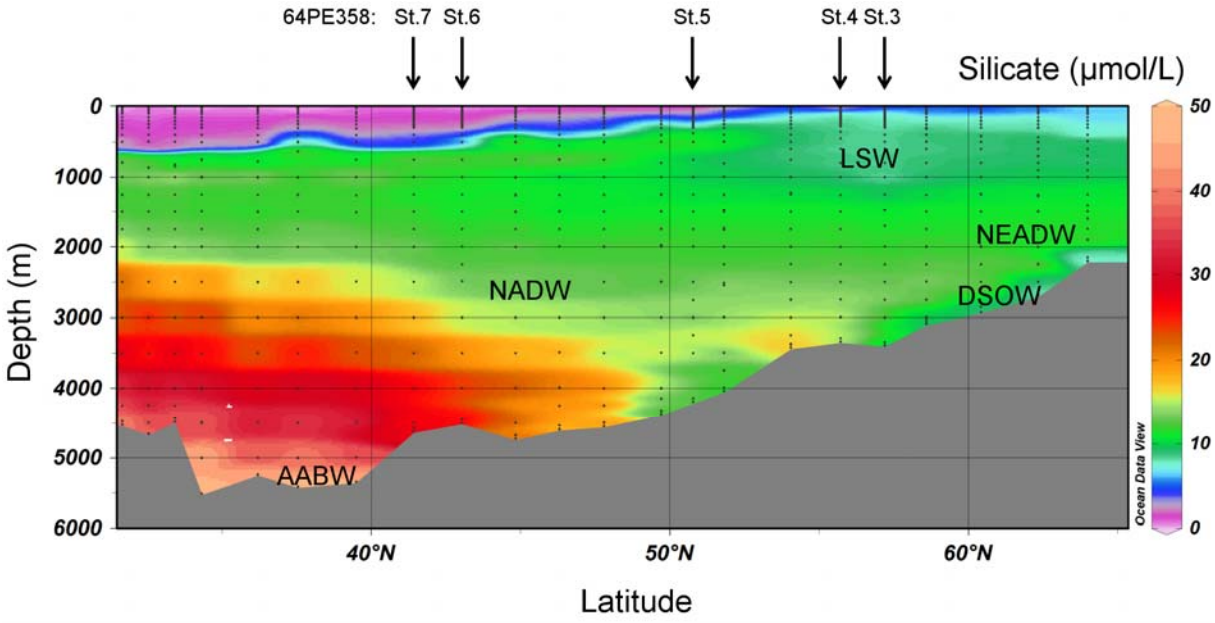

Figure 7. The full western North Atlantic GEOTRACES transect of silicate between Iceland and Bermuda with the stations visited during 64PE358 indicated. Data: Sharyn Ossebaar.

A transect of shallow stations (280 m) was sampled on our way back to Texel. On board measured parameters salinity, temperature, the nutrients phosphate, nitrate and silicate all show a clear distinction between stations 6-7 sampled in the Warm Gulf Stream and stations 9-13 sampled in the northern part of the subtropical gyre (pers. comm. Hendrik van Aken, Royal NIOZ). These ocean areas were separated by the anomalous station 8 with low

salinities, cold temperatures and high nutrient concentrations (Figures 8, 9, 10, 11, 12). The low saline and cool waters of station 8 most likely indicated a cyclonic eddy originating south of Newfoundland where the Warm Gulf Stream and shelf waters including the Labrador Current meet (pers. comm. Hendrik van Aken, Royal NIOZ). That we may have observed an cyclonic eddy here is further confirmed by altimetry, see section 4.2.A.3. In addition, along this transect nitrite maxima coincided with fluorescence maxima indicating the excretion of nitrite by phytoplankton during nitrate reduction (Al-Qutob et al., 2002) (Figures 13 and 14).

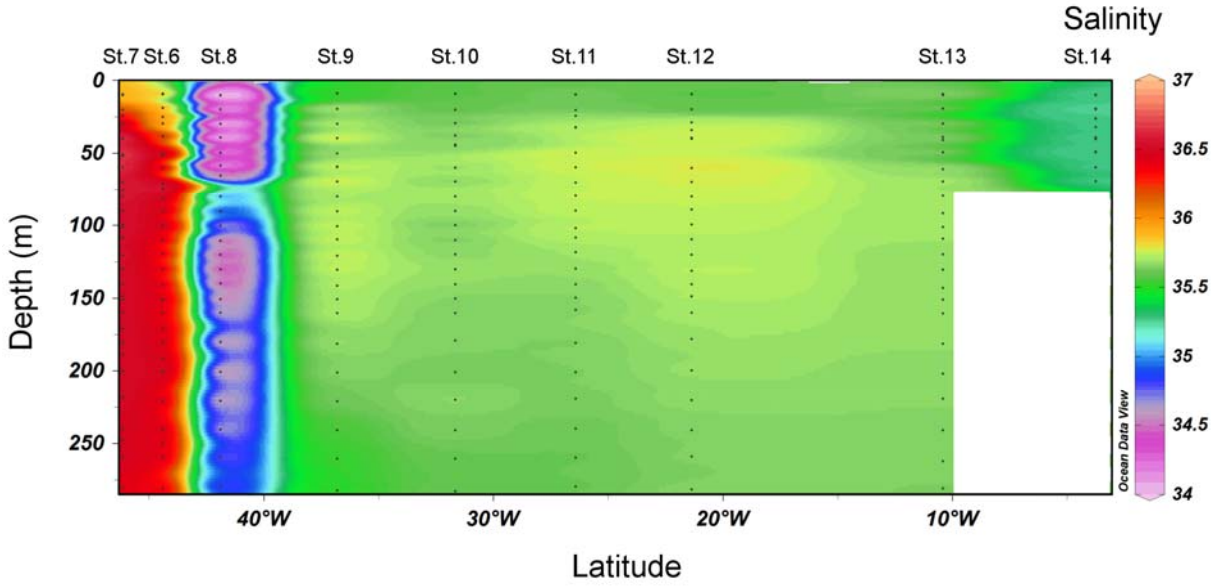

Figure 8. Section plot of salinity along a transect of shallow stations (280 m) between station 7 and station 14 during 64PE358. Data: Sven Ober.

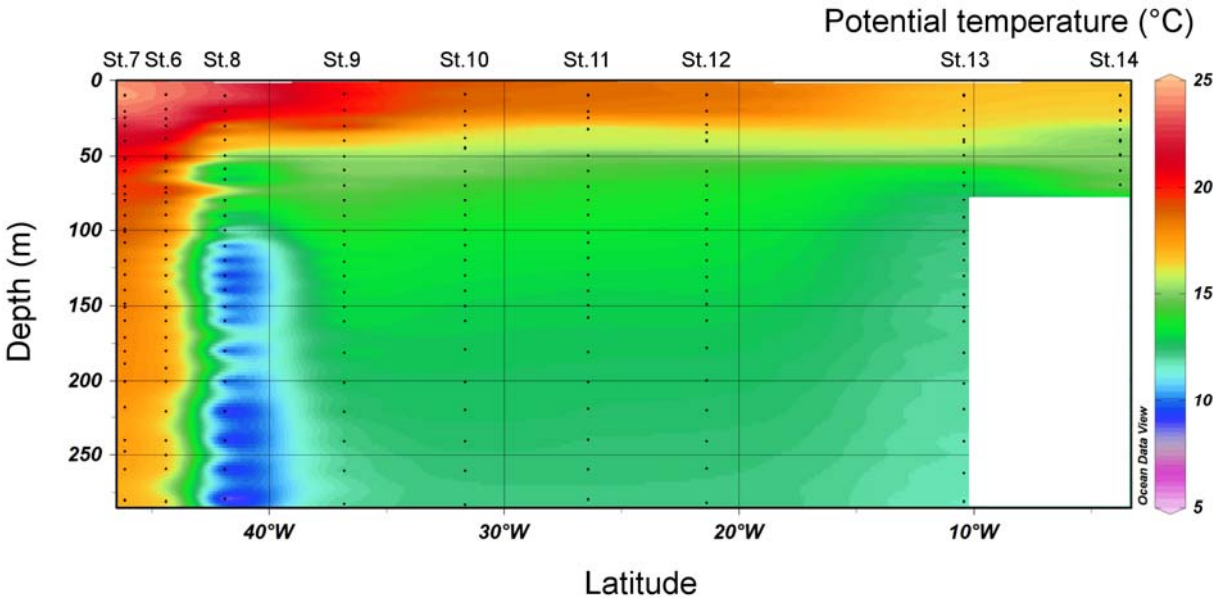

Figure 9. Section plot of potential temperature along a transect of shallow stations (280 m) between station 7 and station 14 during 64PE358. Data: Sven Ober.

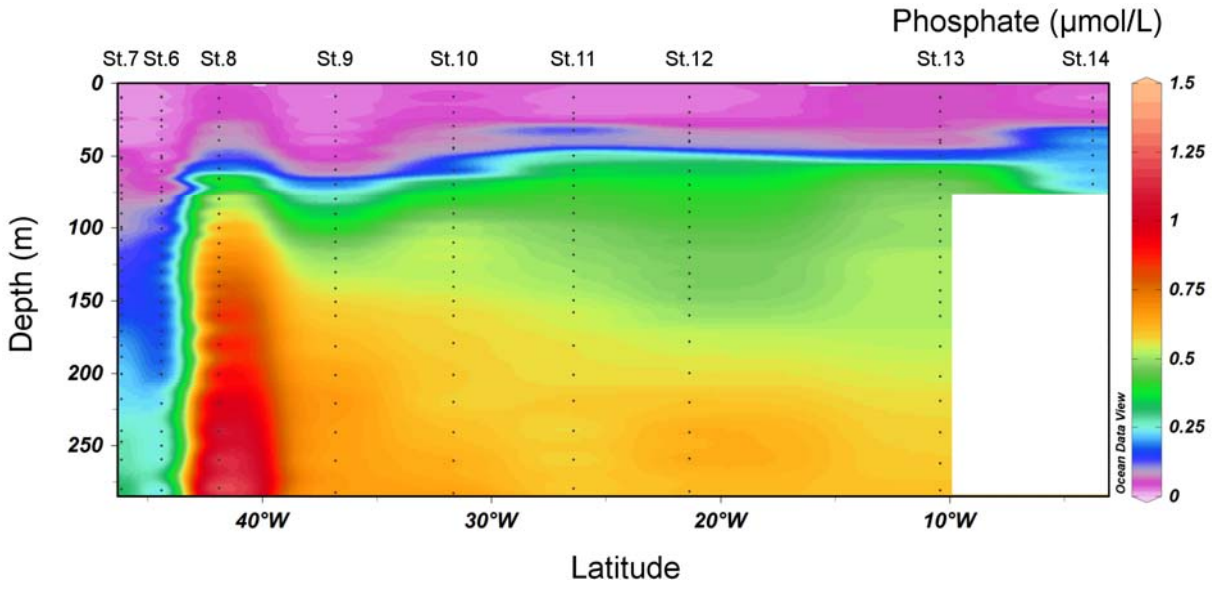

Figure 10. Section plot of phosphate along a transect of shallow stations (280 m) between station 7 and station 14 during 64PE358. Data: Sharyn Ossebaar.

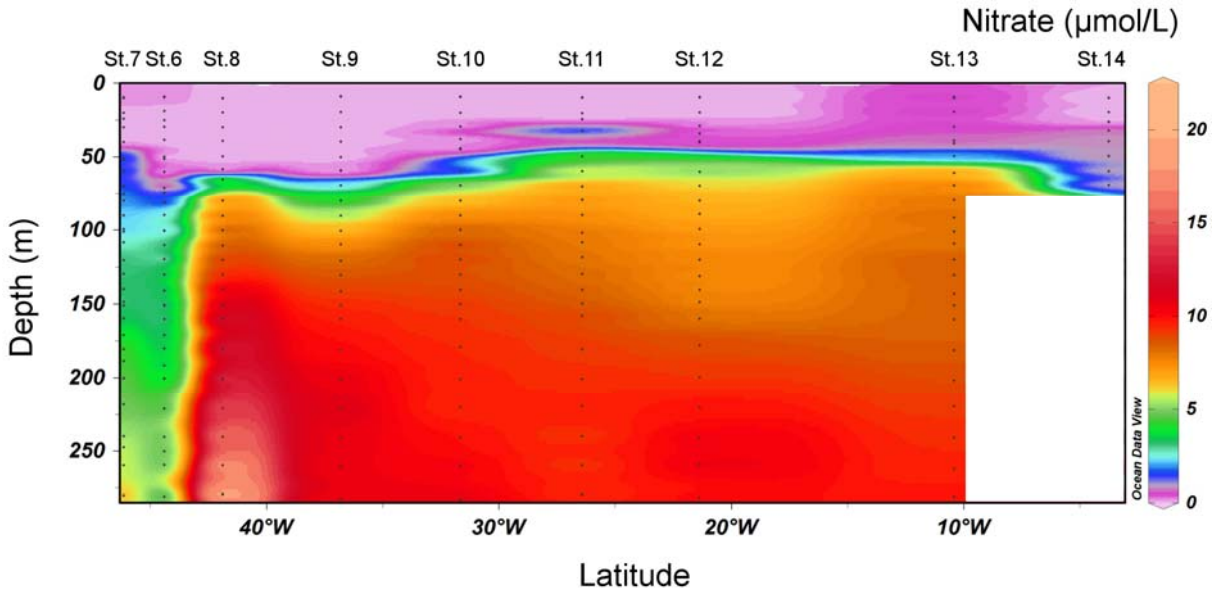

Figure 11. Section plot of nitrate along a transect of shallow stations (280 m) between station 7 and station 14 during 64PE358. Data: Sharyn Ossebaar.

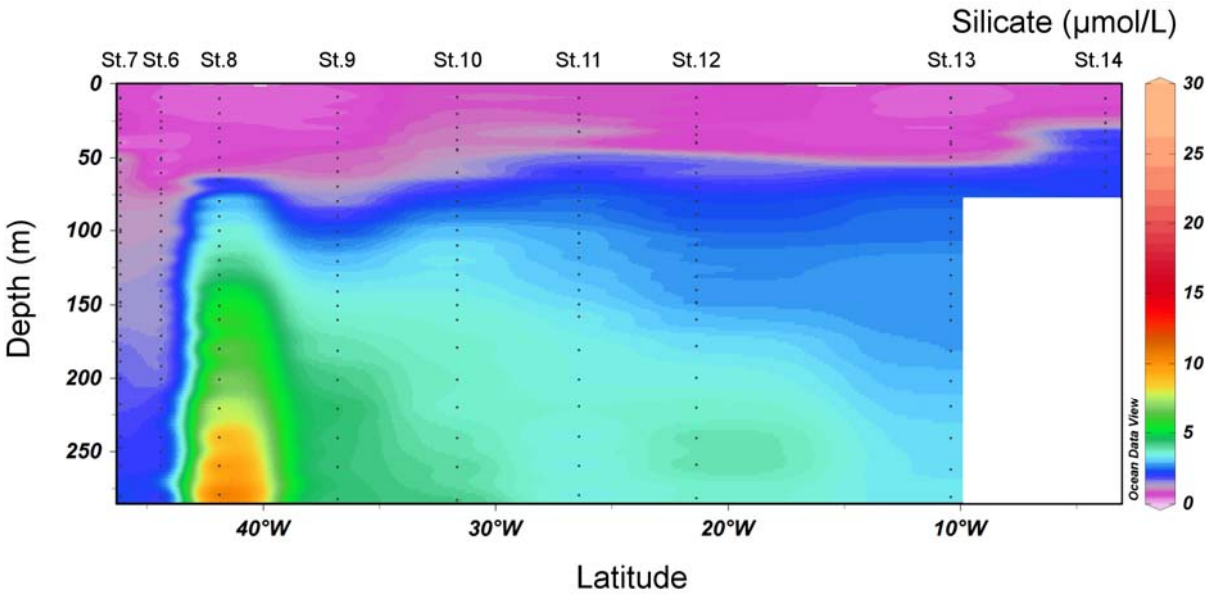

Figure 12. Section plot of silicate along a transect of shallow stations (280 m) between station 7 and station 14 during 64PE358. Data: Sharyn Ossebaar.

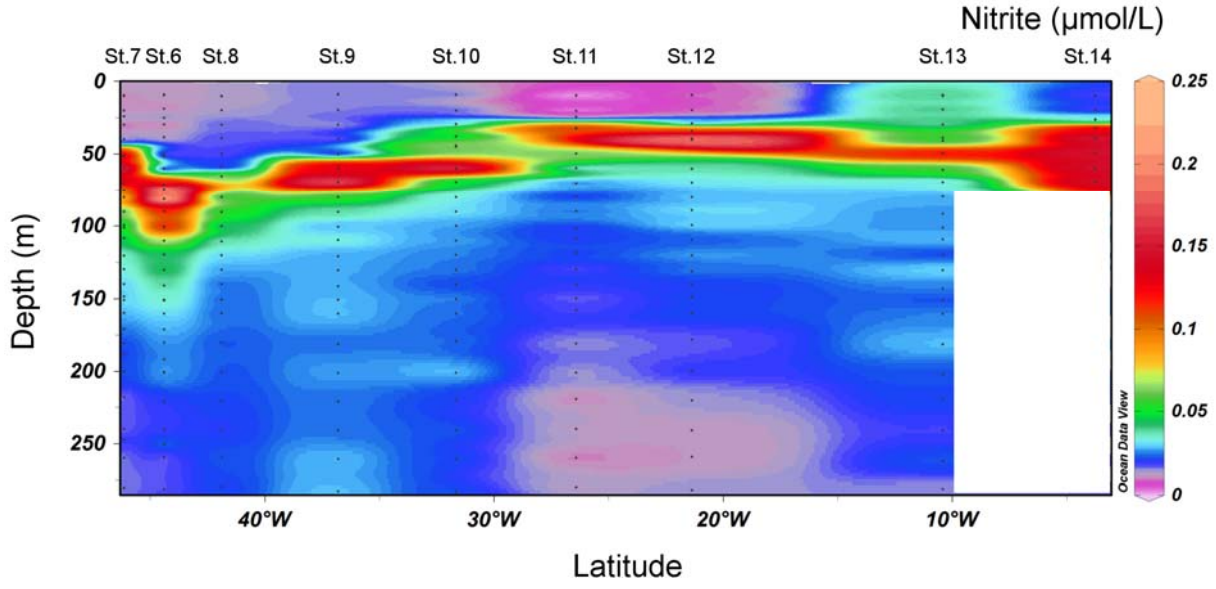

Figure 13. Section plot of nitrite along a transect of shallow stations (280 m) between station 7 and station 14 during 64PE358. Data: Sharyn Ossebaar.

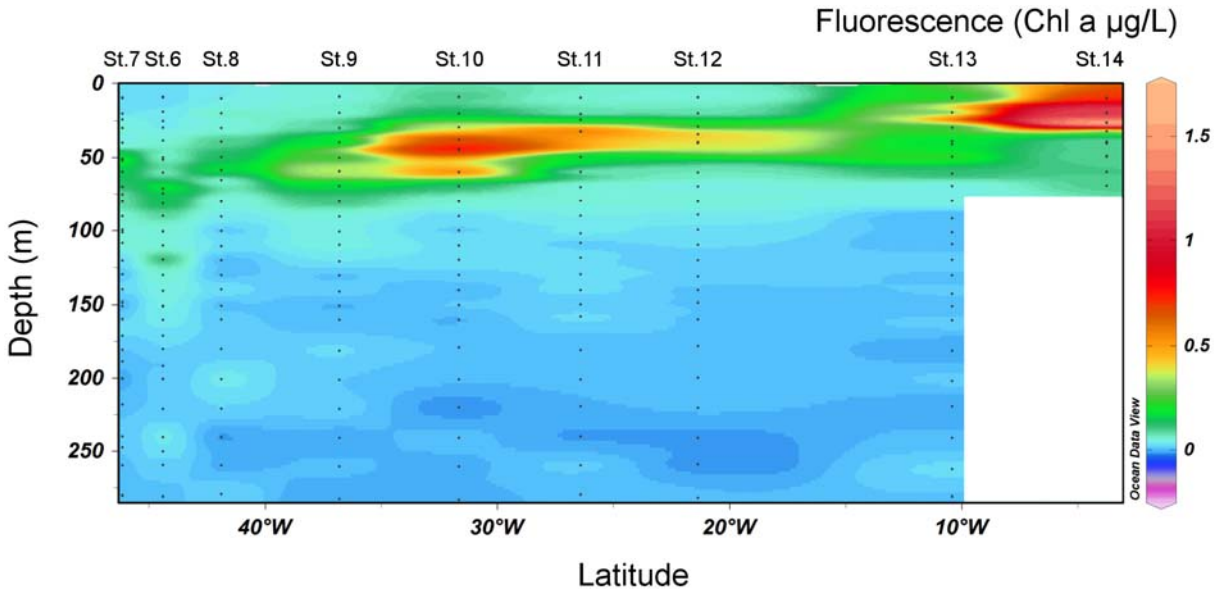

Figure 14. Section plot of fluorescence along a transect of shallow stations (280 m) between station 7 and station 14 during 64PE358. Data: Sven Ober.

Underway surface data

Figure 15 shows the underway surface seawater data as measured by the ship's Aqua flow system (Chelsea Instruments). The sea surface temperature increases southwards (st. 3-7 in Figure 15 a) and westwards (st. 7-14 in Figure 15 b) towards the Warm Gulf Stream. The salinity decreases southwards as the influence of the less saline Labrador current increases (Figure 15 c). The less saline surface waters of the eddy like feature at station 8 (Figure 15 d) was clearly recognizable in the seasurface salinity between station 7 and 14. The seasurface fluorescence between station 3-7 was highest above 52.5°N (Figure 16 a). The seasurface fluorescence between station 7 and 14 increases in eastern direction (Figure 16 b).

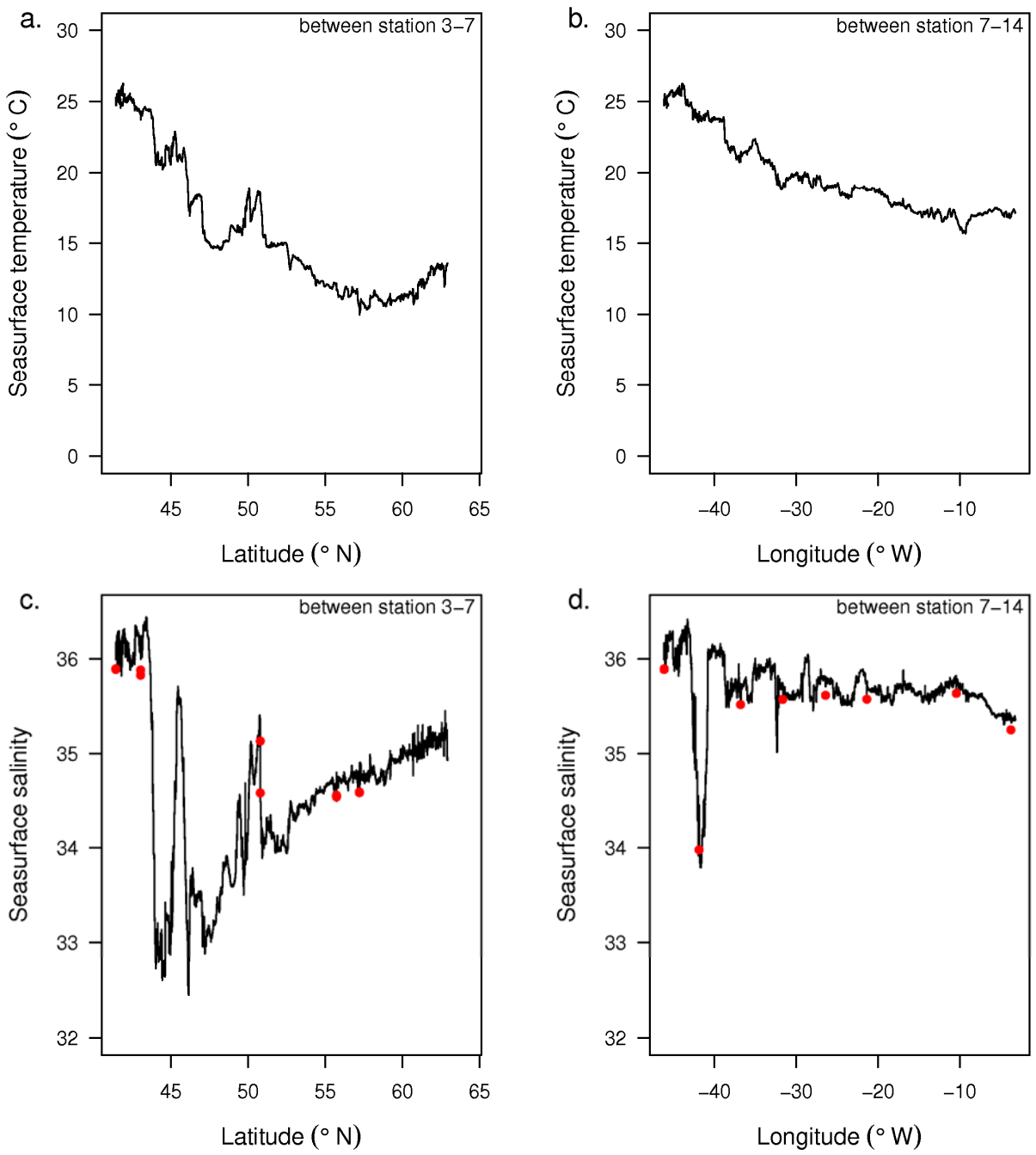

Figure 15. The preliminary uncorrected surface data as measured with the ship's underway system, with: a) the surface seawater temperature between station 3 and 7, b) the surface seawater temperature between station 7 and 14, c) the surface seawater salinity between station 3 and 7, and d) the surface seawater salinity between station 7 and 14. The red dots in c and d represent the preliminary uncorrected salinity measured by the UCC CTD at 10 m depth.

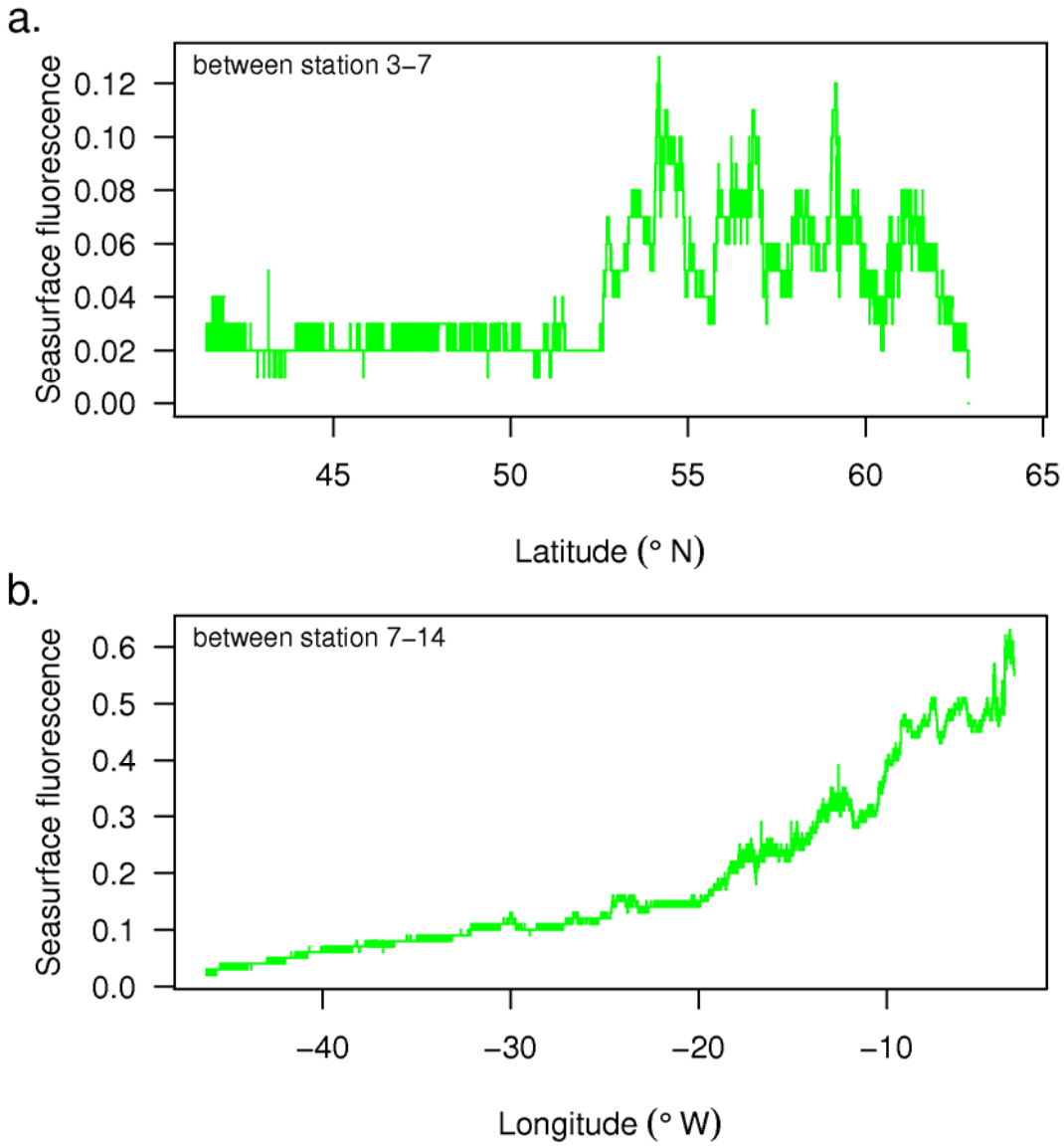

Figure 16. The preliminary underway surface seawater fluorescence data between station 3 and 7 (a.) and station 7 and 14 (b.).

Description of sample equipment and deployment

We used a system for ultra clean trace metal sampling consisting of an all-titanium frame with 24 sample bottles of 27 L each made of PVDF plastic (abbreviated UCC). A Kley France winch was used to deploy the UCC to deep ocean waters by a 17.7 mm diameter Kevlar hydrowire with seven independent internal signal/conductor cables (Cousin Trestec S.A.), see cover picture. Sampling of the UCC occurred in a class 100 clean-room container (de Baar et al., 2008). Filtered samples were directly filtered from the UCC sample bottles under nitrogen pressure using 0.2 µm Sartobran 300 cartridges (Sartorius).

To collect low Fe surface seawater for use in the laboratory we pumped seawater into a trace metal clean laboratory container using a Teflon diaphragm pump (Almatec A-15, Germany) connected by a braided PVC tubing to a towed fish positioned at approximately 3 m depth alongside the ship. This surface seawater from the fish was filtered in-line using a

Sartobran 300 filter capsule (Sartorius) with a 0.2 μm cut-off and subsequently stored in a cubic meter vessel.

Concluding

By sampling the full depth water column at station 3-7 we now filled up the gaps in the northern part of our western Atlantic GEOTRACES transect. To elucidate the internal cycling of Fe, Co, Zn and Cd in the upper 300 m we performed 10 high resolution shallow casts measuring the fine scale distribution of DFe, colloidal Fe, truly dissolved Fe, organically complexed Fe and size fractionated Co, Zn and Cd with respect to phytoplankton abundance (fluorescence) and the physical oceanography in the upper water column. Photo-acclimation and phytoplankton community composition were investigated at 12 stations and the CO_2 system was investigated at the 5 full depth GEOTRACES stations and an additional 7 high resolution shallow stations. At the GEOTRACES stations additional samples were taken for the organic complexation of cobalt (Co), silver (Ag), arsenic (As) and antimony (Sb), Cd isotopes (station 5), and $^{14}C/^{13}C$ (stations 4, 5 and 6). Furthermore, we successfully recovered and serviced the LOCO2 mooring.

References

Al-Qutob, M., Hase, C., Tilzer, M.M. and Lazar, B., 2002. Phytoplankton drives nitrite dynamics in the Gulf of Aqaba, Red Sea. Marine Ecology-Progress Series, 239: 233-239

de Baar, H.J.W., Timmermans, K.R., Laan, P., De Porto, H.H., Ober, S., Blom, J.J., Bakker, M.C., Schilling, J., Sarthou, G., Smit, M.G. and Klunder, M., 2008. Titan: A new facility for ultraclean sampling of trace elements and isotopes in the deep oceans in the international Geotraces program. Mar. Chem., 111(1-2): 4-21.

1. General introduction of the Netherlands GEOTRACES project

The goal of the GEOTRACES project is to re-visit in 2010-2011 the West Atlantic GEOSECS-1972 cruise to produce complete ocean sections of (A) novel trace elements and several isotopes, (B) transient tracers of global change, (C) microbial biodiversity and metabolism, and (D) interpretation by ocean modelling where the ocean observations A-C serve for verification of the models.

Many of these 'tracers in the sea' are the first-ever ocean sections (sub-projects A, (B), C), while others (sub-project B) will allow unravelling of transient global changes over the past ~35 years by comparison with data of 1972-1973 GEOSECS and later cruises (notably 1981-1983 TTO, WOCE 1990's; CLIVAR).

A) Trace elements and isotopes of the international GEOTRACES program

The first-ever high resolution Atlantic deep section of trace metals Fe, Al, Zn, Mn, Cd, Cu, Co, Ni, Ag were sampled, in conjunction with lower resolution sampling for Rare Earths, natural isotopes ^{234}Th, ^{230}Th, ^{231}Pa, ^{223}Ra, ^{224}Ra, ^{226}Ra, ^{228}Ra, ^{227}Ac and anthropogenic isotopes ^{129}I, ^{99}Tc, ^{137}Cs, $^{239,240}Pu$, ^{238}Pu.

More than thirty years after GEOSECS the techniques for ultraclean sampling in a time efficient manner (De Baar et al., 2008) and final analyses have improved enormously.

Nowadays it is feasible to determine for the first time ever the oceanic distributions of key trace metals, other trace elements, and various isotopes, along ocean sections throughout the full 4-6 km depth of the oceans. In the GEOTRACES Science Plan (www.geotraces.org) we have defined 6 key trace metals Fe, Al, Zn, Mn, Cd, Cu, which, together with additional metals Co, Ni, Ag is investigated with high priority in the GEOTRACES West Atlantic Ocean sections. The distribution and biological availability of Fe is strongly controlled by its physical-chemical speciation within seawater, where colloids and Fe-organic complexes are dominant actors. For phytoplankton growth, Cu at the cell wall acts in reductive dissociation of Fe-organic complexes, hence facilitates Fe uptake. This may partly explain the nutrient-type distribution of Cu in the oceans. The external sources of Fe into the oceans are either from above (dust) and below (sediments) and will be constrained by Al and Mn for aeolian dust input and sedimentary redox cycling sources, respectively. Iron enhances phytoplankton growth, which in turn controls the biological pump for uptake of CO_2 from the atmosphere. Due to fossil fuel burning the CO_2 also increases in ocean waters and this may affect phytoplankton ecophysiology, with key links of metals Fe and Zn in overall photosynthesis and in carbonic anhydrase, respectively, where Cd and Co may substitute for Zn in the latter carbonic anhydrase.

B) Global change of anthropogenic CO_2 invasion and other transient anthropogenic tracers

Water masses, circulation and mixing are defined by classical S, T, p combined with datasets of dissolved nutrients and O_2, as well as transient tracers DIC, CFCs, novel SF6, $^3H/^3He$ and $^{13}CO_2$, $^{14}CO_2$ also to derive 'ages' of a water mass. The invasion of transients is mostly in the North Atlantic Ocean and partly overlaps with warming of upper ocean waters, and with the increase of CO_2 inventory, hence ocean acidification.

Aim is the determination of anthropogenic CO_2 inventory by measurements of DIC, Alkalinity and transient radiocarbon, and interpretation relying also on other transients (CFC's; SF6; $^3H/^3He$; other noble gases) measured by international partners. The overarching hypothesis is the very obvious statement: **The best possible estimate of the inventory of anthropogenic CO_2 in the Atlantic Ocean can be achieved by optimizing between a suite of transient tracers and approaches, for optimal concordance between them.**

The first major objective is to quantify the inventory of anthropogenic CO_2 along the transect in the West Atlantic Ocean by a suite of different approaches, as follows:
(i) simple (or simplistic) comparison of DIC inventories over the period between 1981-1983 and 2009-2010, as to derive an inventory increase over this circa three decades time interval;
(ii) instantaneous back calculations using DIC, nutrients, O_2, by several methods like delta C*, TROCA, eMLR;
(iii) combinations of DIC data and one or more transient tracers.

Each one of these approaches requires insight and skill, but is in itself quite feasible to pursue. Afterwards these various findings will be evaluated, and the most promising approaches will be applied for an expansion both in time and in space, by developing a time history of increasing anthropogenic CO_2 inventory in the complete North Atlantic Ocean basin, also relying on preceding data in the CARINA database. This expansion towards a basin wide estimate will be in conjunction with the sub-project D. global ocean modelling.

C) Microbial oceanography: biodiversity and turnover rates of prokaryotes, eukaryotes and viruses

Biodiversity, abundance and metabolic rates of microbes (eukaryotes, prokaryotes and viruses) were determined in the meso- and bathypelagic ocean. Particularly, the role of chemoautotrophy in the deep ocean is investigated as it might represent an unrecognized source of dark ocean 'primary productivity'.

The main objective of the proposed study is to mechanistically understand the dynamics in diversity and function of the meso- and bathypelagic food web in relation to hydrodynamic conditions in distinct deep-water masses of the North Atlantic and at water-mass boundaries where diversity hotspots are expected to occur as predicted by the ecotone concept. The main objective translates into the following **specific objectives**:

i) To link phylogenetic prokaryotic diversity to selected prokaryotic functions relevant for the dark ocean's biogeochemical fluxes (remineralisation of organic matter, organic matter production, ectoenzymatic activity, etc.) using a combination of approaches.

ii) To differentiate between the distribution of abundant and rare prokaryotic taxa and to determine the significance of rare taxa for the functioning of the community.

iii) To determine the extent of the recently discovered archaeal chemoautotrophy in the meso- and bathypelagic realm.

iv) To relate dynamics in abundance and activity of the dark ocean biota to changes in the quantity and quality of the organic matter, water mass age and remineralisation activity.

v) To determine the expression of selected functional genes for Archaea and Bacteria indicative of major metabolic pathways using targeted Q-PCR analyses in specific deep-water masses.

vi) To assess the role of viruses as compared to protists as consumers of prokaryotes.

The overarching hypothesis is that the seemingly homogenous water column of the dark ocean is highly structured due to the hydrodynamics of the different water masses. Each water mass carries its specific biogeochemical characteristics and allows the expression of distinct diversity and function patterns of the dark ocean biota. At the interface and mixing zones of deepwater masses, persistent deep-sea ecotones exist, representing 'hotspots' in diversity and activity of microbes with significant influence on the overall biogeochemical cycles of the dark ocean.

D) Ocean Biogeochemical Climate Modelling

The above datasets A,B,C are in mutual support and moreover combine to serve for Ocean Biogeochemical Climate Modelling towards more rigorous, integrated understanding of processes including the role of the Atlantic Ocean in global change.

References

de Baar, H.J.W., Timmermans, K.R., Laan, P., De Porto, H.H., Ober, S., Blom, J.J., Bakker, M.C., Schilling, J., Sarthou, G., Smit, M.G. and Klunder, M., 2008. Titan: A new facility for ultraclean sampling of trace elements and isotopes in the deep oceans in the international Geotraces program. Marine Chemistry, 111(1-2): 4-21.

2. Participants and parameters

2.1. List of participants

1	**Micha Rijkenberg PI**	NIOZ; BIO-Chemical Oceanography
2	**Nikki Clargo**	NIOZ; BIO-Chemical Oceanography
3	**Gabriel Dulaquais**	LEMAR IUEM
4	**Audrey van Mastrigt**	University of Groningen
5	**Sven Ober**	NIOZ; FYS
6	**Sharyn Ossebaar**	NIOZ; MRF
7	**Jack Underwood**	University of Utrecht
8	**Sophie Vergouwen**	University of Groningen
9	**Leon Wuis**	NIOZ; MTEC

For complete addresses and email see Appendix 1

Figure 17. Scientists and crew during 64PE358 on the RV Pelagia in the western North Atlantic Ocean.

2.2. UCC Sample Team

The following people have been part of the general UCC sampling team in the ultraclean container:

1) Micha Rijkenberg
2) Gabriel Dulaquais
3) Audrey van Mastrigt
4) Sophie Vergouwen

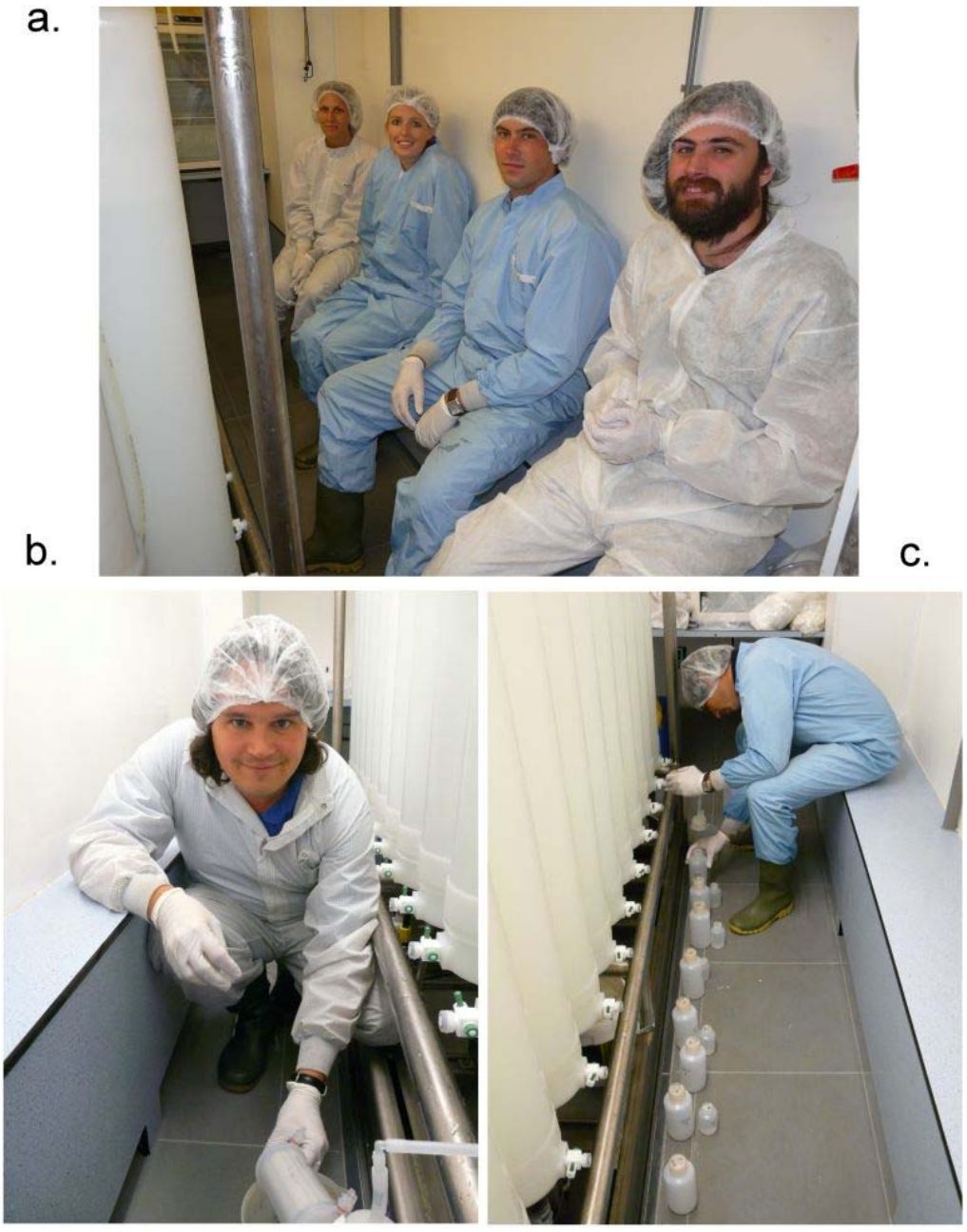

Figure 18. a) Sophie, Audrey, Gabriel and Jack, b) Micha, and c) Gabriel sampling in the ultra clean container.

2 .3. List of parameters

Samples	collected by	responsible for analysis and data
UC CTD (UCC)		
Library metals totals	M. Rijkenberg	P. Laan, M. Rijkenberg, H. de Baar
Library metals dissolved[1]	M. Rijkenberg	R. Middag, P. Laan, M. Rijkenberg, H. de Baar
Nutrients	S. Ossebaar	S. Ossebaar
Dissolved Fe	M. Rijkenberg	P. Laan, M. Rijkenberg
Fe ultra filtration	M. Rijkenberg	P. Laan, M. Rijkenberg
Fe Speciation	M. Rijkenberg	L. Gerringa
Fe speciation	M. Rijkenberg	S. van den Berg
Dissolved Ag	M. Rijkenberg	E. Achterberg
Dissolved As, Sb	M. Rijkenberg	P. Salaun
Dissolved Co, Zn, Cd	G. Dulaquais	G. Dulaquais, M. Boyé
Co-speciation	G. Dulaquais	G. Dulaquais, M. Boyé
Co, Zn, Cd ultrafiltration	G. Dulaquais	G. Dulaquais, M. Boyé
Total dissolvable Co, Zn, Cd	G. Dulaquais	G. Dulaquais, M. Boyé
Dissolved Cd isotopes	M. Rijkenberg	W. Abouchami
Phytoplankton DNA	A. van Mastrigt/S. Vergouwen	W. van de Poll
Phytoplankton pigments	A. van Mastrigt/S. Vergouwen	W. van de Poll
Phytoplankton photosynthetic parameters	A. van Mastrigt/S. Vergouwen	W. van de Poll
$^{14}C/^{13}C$	A. van Mastrigt/S. Vergouwen	S. van Heuven, H. Meijer
Salinity	S. Ober	S. Ober
O_2	S. Ossebaar	S. Ossebaar

[1] Rob Middag will use the chelating resin Nobias-chelate PA1 in an off-line pre-concentration manifold with magnetic sector inductively coupled plasma mass spectrometry (ICP-MS) detection for analysis of Y, Cd, La, Pb, Sc, Ti, V, Mn, Fe, Ni, Zn and Ga.

3. Recovery, servicing and redeployment of the LOCO2 Mooring

Sven Ober[1], Leon Wuis[1] and Jack Underwood[2]

[1] Royal Netherlands Institute for Sea Research, Texel, the Netherlands
[2] University of Utrecht

On Aug 1st the mooring LOCO2-9 was recovered (Figure 19). Unfortunately the main instrument, a McLane Moored Profiler, didn't work properly. At the moment it is unknown what went wrong. Analysis of the log-files with help and advice from the manufacturer will hopefully clarify this. The other instruments: 2 ADCP's and a SBE37 moored CTD, were still working after the recovery. They were stopped by software commands and the data was uploaded to computers with a back-up to the ships network. After the recovery of the mooring a full depth CTD-cast was carried out exactly on the mooring position, mainly for calibration purposes.

In the afternoon of Aug 2nd the mooring LOCO2-10 has been deployed. The instruments for LOCO-10 were prepared during the preparation of the cruise at NIOZ. Prior to the deployment of the mooring, the instruments were started in the usual way: Sven Ober carried out the start-up procedures and his work was checked and logged by a second person, in this case Jack Underwood. The weather conditions were near perfect and the deployment went smooth. The position of LOCO2-10 is: 59°12.32' N 39°30.47' W. After the deployment a full depth CTD-cast was carried out at a distance of 1 nautical mile from the position of the mooring. These CTD-data will be used for inter-calibration of the CTD-sensors and the newly deployed mooring sensors. All bottles were closed at about 810 m and were sampled after the cast to check the samplers for any contamination of Fe.

Figure 19. Leon and Sven during the recovery of the LOCO2 mooring.

4. Analyses and measurements

4.1. General parameters

4.1.1. The Ultra Clean CTD-system

Sven Ober[1], Leon Wuis[1] and Jack Underwood[2]

[1] Royal Netherlands Institute for Sea Research, Texel, the Netherlands
[2] University of Utrecht

Description of the UCC-system

The system consists of 3 major modules:

- A box-shaped titanium CTD frame with 24 GoFlo-sampling bottles
- A clean air container for contamination-free (sub)sampling
- A special deep sea winch with a Dyneema CTD-cable

To avoid trace metal contamination the frame of the UCC- system and all electronic pressure housings were made of titanium or clean plastics like Teflon, PVDF or POM. To prevent contamination and to keep the UCC safe and secure the UCC was at all times placed inside the clean air container (meeting class 100 clean-room specifications) when not in use during casts. Prior to a cast the frame was prepared inside that container and transported to the CTD-launching spot using a custom made aluminum pallet and a longbedded forklift. After the cast the UCC was immediately returned to the clean air container to avoid contamination of the equipment with grease, rust or smoke particles from the ship. The electronic CTD sensor system consists of a SBE9plus underwater unit, a SBE11plusV2 deck unit, a NIOZ developed multivalve bottle-controller, a SBE3plus thermometer, a SBE4 conductivity sensor, a SBE5T underwaterpump, a SBE43 dissolved oxygen sensor, a Chelsea Aquatracka MKIII fluorometer, a Wetlabs C-Star transmissiometer (25 cm, deep, red). For Ultra Clean water sampling 24 samplers (27 liter each) were used. These samplers were produced by NIOZ and are made of PVDF and titanium. Due to the butterfly-type closure on both ends of the sampler the opening is maximized resulting in an excellent flow-through. Opening and closing of the samplers are controlled by a hydraulic system. The heart of the sampling system is the NIOZ developed Multivalve. For bottom-detection 2 devices were installed: a Benthos PSA-916 altimeter and a bottom switch with a weight. The SBE11+ has a NMEA interface for navigational data. On the logging computer Seasoft for Windows is installed (Seasave V7.20 and SBE Data Processing V7.20). For calibration of the profiling thermometer (SBE3) a high-accuracy reference-thermometer (SBE35) was mounted.

Functioning of the UCC-system

During the cruise the NIOZ Ultra Clean CTD-system (UCC) was used for ultra clean trace metal sampling (Figure 20). The UCC-system was deployed 21 times including a test cast. A problem with the duct of the CTD during the test cast prevented the collection of sensor data.

As a consequence the test cast was only successfully used to test the sampling system which worked flawless. The problem with the duct was solved. During the next 2 casts the DO-sensor including the interconnecting cable showed some strange contact problems and had to be changed. The transmissiometer stopped working for an unknown reason during Station 1 cast 2 and had to be changed as well. Both instruments were serviced very recently by the manufacturers and will be returned for warranty-repairs. During Station 6, Cast 1 the interconnecting cables of the conductivity sensor showed contact problems. The sensor worked fine after replacing this cable. The rest of the cruise all sensors including a refurbished altimeter worked perfectly. The sampling system worked flawless from start to end.

The system was equipped with a SBE-35 reference-thermometer for in situ calibration of the SBE-3 profiling thermometer. A first analysis of the temperature calibration data showed that on average the output of the SBE3 was 1.5 mK too high with a standard deviation of 0.8 mK based on 51 measurements.

36 Salinity-samples were collected from the deep casts and analyzed on board with a Guildline 8400B Autosal using OSILS standardwater batch P150. The average difference between the salinity measured with the Autosal and the CTD was 0.0003 with a standard deviation of 0.0011. Not a single sample had to be rejected.

Dissolved oxygen (DO) samples were collected from the deep casts and measured using Winkler titrations in order to calibrate the DO-sensor. A first analysis of the Winkler results has not been finished yet due to a software problem. This software problem can be solved on shore easily. The CTD DO-sensor behaved good during the casts.

a.

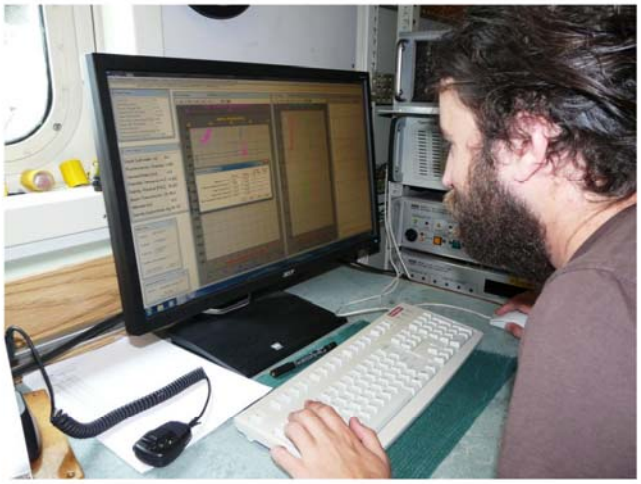

b.

Figure 20. a) Jack closes the bottles of the UCC frame during the up cast, and b) Leon operates the Kley France winch.

4.1.2. Dissolved oxygen

Sharyn Ossebaar

Royal Netherlands Institute for Sea Research, Texel, the Netherlands

Dissolved oxygen was measured from four depths from each CTD cast to check the calibration of the oxygen sensor fixed to the CTD frame itself. A refined protocol of the spectrophotometric Winkler approach was conducted, where a continuous-flow analyzer is coupled with a custom-made autosampler holding up to 30 oxygen bottles (Reinthaler et al. 2006). The time required for analysis is 2 min per sample, and the precision is 0.05% at ~200 mmol O_2 m^{-3}. Dissolved oxygen was analysed in a thermostated lab container equipped with a Traacs 880 auto-analyser spectrophotometer measuring the intense yellow colour of the samples produced from the formation of iodine after the addition of acid. 25 samples were analysed for the cruise. All measurements were calibrated with standards diluted in oxygen saturated surface sea water in the salinity range of the Atlantic Ocean stations.

Theory and Method
For the measurement of dissolved oxygen in the water column a refined protocol of the spectrophotometric Winkler approach (Winkler, 1888) was conducted in combination with a Traacs auto-analyser spectrophotometer. This method is based on the following redox-reactions:

$$2\ Mn^{2+} + 4\ OH^- \rightarrow 2\ Mn(OH)_2 \quad (1)$$

$$2\ Mn(OH)_2 + O_2 \rightarrow 2\ MnO(OH)_2 \quad (2)$$

$$2\ MnO(OH)_2 + 8\ H^+ + 6\ I^- \rightarrow 2\ Mn^{2+} + 2\ I_3^- + 6\ H_2O \quad (3)$$

$$2\ I_3^- + 2\ S_2O_3^{2-} \rightarrow 6\ I^- + S_4O_6^{2-} \quad (4)$$

In the Winkler method, manganese chloride is added to a known amount of seawater, followed by the addition of an alkaline sodium hydroxide-potassium iodide solution. The Mn^{2+} is oxidized by the dissolved oxygen to higher oxidation states resulting in a manganous hydroxide ($MnO(OH)_2$) precipitate in the water and forms a hydrated tetravalent oxide of manganese. Upon acidification, the manganese hydroxides dissolve to reduce the manganese back to the Mn^{2+} form and the tetravalent manganese acts as an oxidizing agent which liberates iodine in the form of I_3^- ions from the iodide ions, which has an intense yellow colour. The iodine is equivalent to the dissolved oxygen in seawater and present as free iodine (I_2) and tri-iodide (I_3^-). The color of the sample is determined by the light transmission through the sample-bottle with a spectrophotometer and is based on measuring the absorbance of the colored I_2 and I_3^-. The concentration of oxygen is then calculated by comparing the absorbance in a sample against standards of known oxygen content made from potassium iodate (KIO_3) solutions.

Equipment
For the dissolved oxygen analysis, a custom-made autosampler was used in combination with a standard Technicon TRAACS 800 autoanalyzer (Bran + Luebbe, Germany). The

autosampler consists of an electric motor, a pneumatic sampling arm driven by compressed air at ~5 bar, and a magnetic stirrer. The parameters were adjusted to 30-s flushing with wash solution, followed by 3 picks of a sample and 90-s aspiration of the sample. The platform holds up to 30 bottles, and the autosampler is completely independent from the TRAACS analyzer and its software. The TRAACS analyzer was equipped with a standard tungsten filament lamp and a fixed band pass filter of 460 ± 10 nm. The flow cell had a volume of 7.85 mm^3, and the flow rate was set to ~1 cm^3 min^{-1} via the internal peristaltic pump. To maintain a stable temperature in the flow cell, a heat exchange element was installed in front of the cuvette. The analyzer was controlled via the commercial TRAACS analysis software (AACE version 5.40 for Windows).

Chemicals

The common Winkler reagents were used to determine oxygen concentrations:
Reagent (A): $MnCl_2$; Manganese Chloride ($MnCl_2 \cdot 4H_2O$; 600 g dm^{-3}; 3 mol L^{-1})
Reagent (B): KI/NaOH; Alkaline iodide reagent (NaOH; 250 g dm^{-3}; 6 mol L^{-1} + KI; 350 g dm^{-3}; 2 mol L^{-1})
Reagent (C): $5NH_2SO_4$; Sulfuric acid (H_2SO_4; 10 mol L^{-1})

After preparation, the reagent-grade chemicals were filtered through Whatman GF/F filters and subsequently stored in polycarbonate bottles at ~20°C in the dark. The standard stock solution was prepared with Potassium Iodate (KIO_3) (Malinckrodt Baker; primary standard). KIO_3 was dried at 180°C for 6 h, and 2.5g KIO_3 was dissolved in 250ml ultrapure Milli-Q water. Thus, 1ml KIO_3 stock solution is equivalent to 75.30 mmol O_2 L^{-1}. The prepared stock solution was divided into small 50 ml polycarbonate bottles and stored in a chamber with 100% humidity to prevent evaporation of water and therefore an increase in the concentration of the stock solution over long storage periods.

Glass bottles

Custom-made oxygen bottles made from borosilicate glass with a nominal volume in the range of 116 to 122ml were calibrated to the mm^3 level. Each borosilicate glass bottle and the corresponding ground-glass stopper were engraved with a unique number for later identification of the exact volume. A set of these bottles was used to prepare the calibration standards. In the analysis software of the instrument, we apply a single volume-correction factor calculated from the mean of the volume class, resulting in the automatic output of final oxygen concentrations. Thus, the yellow colored bottles were used during sampling of this cruise with the correction factor of 1.0345 being used.

Sampling

Samples of seawater were obtained from the Ultra Clean CTD sampler from only four depths as a calibration for the oxygen sensor fixed to the CTD frame itself. Seawater was siphoned into the 120 ml oxygen bottles (yellow labeled volume class) with Tygon tubing overflowing each bottle by at least 3 times its volume and the first samples to be sampled from the CTD. The oxygen content in the bottle was fixed as quickly as possible with 1 ml reagent A ($MnCl_2$), followed by 2 ml reagent B (KI/NaOH), both added under the shoulder of the bottle with high-precision dispensers (Fortuna Optifix basic; precision ± 0.1%). The precise addition of chemicals (A) and (B) is important because they dilute the sample. After adding the reagents, the bottles were stoppered and shaken vigorously for approximately 20 sec. to mix the chemicals. The stoppering of the bottles were done as quickly as possible to prevent

contamination of undersaturated samples by atmospheric oxygen and an elastic band ensured that the stopper remained well in place. The bottles were stored immersed in water baths (kept at in situ container temperature) to avoid drying of the stopper seal. After approximately 20 mins, the fixed bottles were shaken again to ensure complete reaction of the chemicals. Samples are needed to be stored under water for at least 2 hours after the second shaking. Samples were measured a few days later. Before starting the measurements on the TRAACS system, 1ml of reagent (C) (5NHCl) was added to the fixed samples. Subsequently, a small magnetic stirring flee was introduced carefully, and the bottle openings were covered with parafilm to avoid loss of volatile compounds. The bottles were immediately covered with dark plastic cylinders shielding ambient light as iodine is light sensitive. The samples were gently stirred for a few seconds with an external magnetic stirrer (Metrohm) until the precipitate in the bottles was dissolved. Finally, the bottles were placed on the autosampler. Before aspiration of the sample into the flow-through analyzer, the sample was agitated again with the built-in magnetic stirrer of the auto-sampler to ensure complete mixing of the solution, thereby preventing chemical stratification.

Calibration and Measuring Procedure

Instrument calibration involves the measurement of the baseline or wash solution, a primer, instrument calibration standards, and sensitivity drift standards. For the wash solution and standards used during work at sea, particle-poor oxygen saturated seawater was collected into an 20L polycarbonate carboy and acclimatized at 20°C. For the instrument calibration standards and the primer, seawater was poured into oxygen bottles with known volume. Subsequently, reagents A (1 ml), B (2 ml), and C (1 ml) were added in reverse order with the high-precision dispensers. After the addition of each reagent, the bottles were stoppered and vigorously shaken. Finally, the KIO_3 standard solution was added with highly accurate adjustable volume electronic pipettes. After a magnetic stirring flee was inserted into a bottle, the bottle was immediately covered with parafilm and a dark plastic cylinder. The primer is equal to the highest standard and is used to adjust the baseline and gain setting of the photomultiplier to prevent the sample peaks from going off scale. Generally, calibration was done in the range of expected oxygen concentrations. For flow-through systems, it is necessary to provide a low concentration marker or baseline to separate consecutive peaks. To minimize carryover effects between the baseline and the samples, the wash solution was adjusted to an oxygen concentration slightly lower than the expected lowest value in the samples. The baseline is measured at the start and the end of an analytical run to correct for baseline drift if necessary. To correct for changes in the sensitivity of the photomultiplier (e.g., due to slight temperature variations), sensitivity drift standards were prepared with an O_2 concentration between the highest and lowest sample in the batch. The drift standards were placed after the instrument calibration standards, and at the end of the run. Both wash solution and sensitivity drift standards were prepared similarly to the calibration standards. A conventional blank is not required for calibration because standards and references include all the chemicals also used for regular samples. All preparations and measurements were done in the temperature controlled container set at 20°C. The calibration standards were diluted from the 75.30 mmol L^{-1} stock solution and were freshly prepared. The calibration of the system gave a correlation coefficient of 0.9999 for 4 calibration points, for linear chemistry. A reference sample with a known oxygen saturation was also measured as a control for the quality of the analytical measurements and were within 1% of its expected value. Duplicate samples were measured from each station to control both the sampling procedure and the reproducibility of the spectrophotometer. The accuracy of the method was 99.7% ± 0.2% as

determined by comparing the measured versus the theoretical oxygen concentration of saturated seawater at 20°C. The measured absorbance of the iodine at 460 nm wavelength is linear up to an equivalent of 350 mmol O_2 L^{-1}, which is within the range of open ocean oxygen concentrations.

References

Reinthaler T. et al 2006. Fully automated spectrophotometric approach to determine oxygen concentrations in seawater via continuous-flow analysis. *Limnol. Oceanogr. Methods* 4, 2006, 358–366

Winkler, L. W. 1888. Die Bestimmung des im Wasser gelösten Sauerstoffes. Chem. Berichte 27:2843-2855.

4.1.3. Nutrients

Sharyn Ossebaar

Royal Netherlands Institute for Sea Research, Texel, the Netherlands

Nutrients were analysed in a thermostated lab container equipped with a QuAAtro Continuous Flow Analyser (Figure 21). The sample rate was set to 60 samples per hour, measuring about 460 samples during the cruise. Measurements were made simultaneously on four channels for phosphate, silicate, nitrite, and nitrate with nitrite together. All measurements were calibrated with standards diluted in low nutrient seawater (LNSW) in the salinity range of the Atlantic Ocean stations and the same LNSW was used as wash water in-between the samples.

Equipment and methods:

Sampling and Measuring

Sample seawater was obtained from the Ultra Clean CTD sampler from all depths. All samples were collected in 125 ml polypropylene bottles after the gases oxygen and TCO2, ^{14}C and salinity sampling. The bottles were rinsed three times with the seawater before being fully filled. In the lab container the nutrient samples were transferred into 5 ml polyethylene vials, (also known as 'ponyvials') after rinsing three times, covered with parafilm against evaporation, and placed in the sampler. All analyses were done within 6 hours on the auto-analyzer, a SEAL QuAAtro autoanalyzer. Calibration standards were diluted from stock solutions of the different nutrients in 0.2µm filtered LNSW and were freshly prepared every day. The LNSW is surface seawater depleted of most nutrients; it is also used as baseline water for the analysis between the samples. Each run of the system had a correlation coefficient of at least 0.9999 for 10 calibration points, but typical 1.0000 for linear chemistry.

The samples were measured from the lowest to the highest concentration in order to keep carry-over effects as small as possible, i.e. from surface to deep waters. Prior to analysis, all samples and standards were brought to lab temperature of 22°C in about one to two hours; concentrations were recorded in 'µmol L^{-1}' at this temperature. During every run a daily freshly diluted mixed nutrient standard, containing silicate, phosphate and nitrate (a so-called nutrient cocktail), was measured in triplicate. Additionally, a natural sterilized Reference Material Nutrient Sample (JRM Kanso, Japan) containing known concentrations of silicate, phosphate, nitrate and nitrite in Pacific Ocean water, was analyzed in triplicate in every run. The cocktail and the JRM were both used to monitor the performance of the analyzer. Finally, the Japan reference material of the batch AX was used to adjust all data to the level of the

known concentrations by means of a correction factor. The final data set is thus referenced to the same Japan reference material values, which makes data comparable and consistent as measured in the previous GEOTRACES cruises from 2010. From every station the deepest sample bottle was sub-sampled for nutrients in duplicate, the duplicate sample-vials were stored dark at 4°C, and measured again in the next run with the upcoming stations, this being for statistical purposes. Approximately 460 samples were analyzed for phosphate, silicate, nitrate and nitrite in total, from all CTD stations.

Analytical Methods
The colorimetric methods used are as follows:

Phosphate reacts with ammonium molybdate at pH 1.0, and potassium antimonyltartrate is used as an inhibitor. The yellow phosphate-molybdenum complex is reduced by ascorbic acid and measured at 880 nm (Riley & Murphy, 1962).
Silicate reacts with ammonium molybdate to a yellow complex, after reduction with ascorbic acid; the obtained blue silica-molybdenum complex is measured at 800 nm. Oxalic acid is added to prevent formation of the blue phosphate-molybdenum (Strickland & Parsons, 1968).
Nitrate plus nitrite (NO_3+NO_2) is mixed with an imidazol buffer at pH 7.5 and reduced by a copperized cadmium column to nitrite. The nitrite is diazotated with sulphanylamide and naphtylethylene-diamine to a pink colored complex and measured at 550 nm. Nitrate is calculated by subtracting the nitrite value of the nitrite channel from the 'NO3+NO2' value (Grasshoff et al, 1983).
Nitrite is diazotated with sulphanylamide and naphtylethylene-diamine to a pink colored complex and measured at 550 nm (Grasshoff et al, 1983).

Calibration and Standards
Nutrient primary stock standards were prepared at the NIOZ.
Phosphate: by weighing Potassium dihydrogen phosphate into a calibrated volumetric PP flask to 1mM PO_4.
Silicate: by weighing Na_2SiF_6 into a calibrated volumetric PP flask to 19.99mM mM Si.
Nitrate: weighing Potassium nitrate into a calibrated volumetric PP flask set to 10mM NO_3.
Nitrite: weighing Sodium nitrite into a calibrated volumetric PP flask set to 0.5mM NO_2.

All standards were stored at room temperature in a 100% humidified box. The calibration standards were prepared daily by diluting the separate stock standards, using three electronic pipettes, into four 100 ml PP volumetric flasks (calibrated at the NIOZ) filled with low nutrient sea water LNSW. The blank values of the LNSW were measured onboard and added to the calibration values to get the absolute nutrient values. Our standards are regularly monitored by participating in inter-calibration exercises from ICES and Quasimeme and even more recently from the RMNS exercise organised by Michio Aoyama MRI/Japan.

Method Detection Limits

The method detection limits were calculated using the standard deviation of ten samples containing 2% of the highest standard used for the calibration curve and multiplied with the student's value for n=10, thus being 2.81. (M.D.L = Std Dev of 10 samples x 2.81)

	M.D.L.(µM/L)	Used measuring ranges µM/L:
PO4	0.008	2.51
Si	0.012	69.15
NO3+NO2	0.011	32.01
NO2	0.006	2.01

Quality Control and Statistics

NIOZ Cocktail

The NIOZ cocktail solution acts as a lab reference and quality control and was made in the NIOZ lab containing phosphate, silicate and nitrate in a solution containing 40 mg Hg_2Cl_2 per liter as a preservative. Every time it was used, it was diluted 250 times with the same pipette and the same volumetric flask for PO4, Si and NO_3 analysis.

Overall statistics computed against the NIOZ Cocktail diluted 250 times, followed by statistics from the Japan Reference Material at a temperature of 22^{o}C.

In between all runs Cocktail1008X250

	PO_4	Si	NO_3+NO_2
Average Value	0.895µM/L	14.123µM/L	13.861µM/L
Stand dev	0.009	0.083	0.061
CV % Full Scale	0.35	0.12	0.19
n	40	40	40

In one run Cocktail1008X250

	PO_4	Si	NO_3+NO_2
Average Value	0.887µM/L	14.126µM/L	13.794µM/L
Stand dev	0.007	0.077	0.023
CV % Full Scale	0.29	0.11	0.07
n	13	13	13

Japan RMNS (Batch AX)

	PO_4	Si	NO_3+NO_2	NO_2
Average Value	1.623µM/L	59.208µM/L	22.403µM/L	0.394µM/L
Stand dev	0.008	0.451	0.126	0.005
CV % Full Scale	0.33	0.65	0.39	0.23
n	34	34	34	34

Data Quality & Remarks

By monitoring the Japanese Reference Nutrient Material (Batch AX) and the NIOZ in-house Lab Cocktail reference (Cocktail1008) it is possible to monitor the performance of the QuAAtro and its analysis.

It is suggested that through diluting the in-house cocktail by means of an electronic pipette and a calibrated flask, a small error of maximum 0.15% is introduced. All data for the GEORTACES leg being Stations 3 -7 were normalized to the JRMNS batch AX as had been done on the previous three legs resulting in a comparable data set. There is however a slight

decline in the average value found for PO4, Si and NO_2+NO_3 compared to the previous three legs of 2010. Thus, the average found JRMNS values were 2.2%, 1.8% and 0.8% lower for PO4, Si and NO_2+NO_3 respectively than the average of the previous three legs. The difference could be due to standards being used as these are made newly on a yearly basis. This will however be discussed within the nutrient group of the NIOZ. The overall JRMNS statistics for in-between runs is 0.015 µM/L for phosphate, 0.199 µM/L for silicate, 0.137 µM/L for Nitrate and 0.005 µM/L for nitrite, this being the average standard deviation of 10 differences between duplicates measured in two different runs. All data for the GEOTRACES Gulf Stream leg being Stations 8-14 were normalized to the NIOZ cocktail resulting in a comparable data set. The overall NIOZ Cocktail 1008 statistics for in-between runs was 0.012 µM/L for phosphate, 0.104 µM/L for silicate, 0.139 µM/L for nitrate and 0.005 µM/L for nitrite, this being the average standard deviation of 17 differences between duplicates measured in two different runs.

References

Grasshoff, K. et al. 1983. Methods of seawater analysis. Verlag Chemie GmbH, Weinheim. 419 pp.

Strickland, J.D.H. and Parsons, T.R., 1968. A pracitcal handbook of seawater analysis. First Edition, Fisheries Research Board of Canada, Bulletin. No 167, 1968. p.65.

Murphy, J. & Riley, J.P., 1962. A modified single solution method for the determination of phosphate in natural waters. Analytica chim. Acta 27, 31-36

Figure 21. Sharyn measures the nutrients nitrate, nitrite, phosphate and silicate

4.2. Sampling of key parameters

A. Metals and isotopes

4.2.A.1. Dissolved, colloidal and truly soluble Fe

Micha Rijkenberg, Patrick Laan

Royal Netherlands Institute for Sea Research, Texel, the Netherlands

Introduction

Iron (Fe) is a critical nutrient for oceanic primary productivity. It's an important element in many proteins, enzymes and pigments. Due to its low solubility, Fe limits phytoplankton growth in large parts of the ocean (Martin and Fitzwater, 1988; de Baar et al. 1990). The trace metal Fe is therefore one of the 6 key elements in the GEOTRACES Science plan. For GEOTRACES we took samples for DFe, total dissolvable Fe (unfiltered acidified seawater samples) and organic Fe complexation at 5 full depth stations. These stations were positioned to fill up gaps in our transect of cruise 64PE319.

Notwithstanding its low solubility concentrations of dissolved Fe (DFe, < 0.2 µm) are higher than predicted by its solubility product alone and vary widely over the water column and across the surface ocean. This variation in DFe concentrations can be explained by i) the chemistry of Fe in the dissolved phase, ii) the proximity of Fe sources, and iii) biological processes (e.g. high DFe at the oxygen minimum).

DFe consists of several distinguishable and measurable fractions such as a truly soluble Fe fraction (Fe(III) and Fe(II)), a truly soluble organically complexed Fe fraction and a colloidal Fe fraction. The distribution of these different chemical forms of Fe may depend on biological factors and the physical oceanography.

We used size fractionation (filters with 0.02 µm pore size) to investigate the distribution of the different size fractions of Fe over the upper water column (0-280 m depth). With this research we are especially interested in the interplay between these different Fe fractions and their relation to changes in environmental conditions.

Work at sea

Samples were taken with the NIOZ high volume ultraclean CTD: 24 novel PRISTINE® ultraclean water samplers of large 27L volume each placed on the titanium sampling frame. The novel samplers with butterfly valves at both ends, are constructed of ultraclean plastic (PVDF; manufactured ultraclean (www.georgfischer.at) for the semi-conductor industry) and some pivotal parts of titanium. The ultraclean CTD was deployed with kevlar hydrowire having internal signal cables.

After recovery, the ultraclean CTD was immediately placed in a clean room container (within the ISO Class 6 clean room requirements) (de Baar et al. 2008). In the clean room, CTD bottles were pressurized (~1 bar) using filtered N_2 and samples for dissolved metals were filtered over a < 0.2 µm Sartobran 300 cartridge (Sartorius).

For ultrafiltration (< 0.02 µm) samples were directly filtered from the UCC CTD bottles under N_2 pressure. The seawater was firstly filtered over a 0.2 µm Sartobran 300 cartridge and subsequently inline ultrafiltered using a Virosart CPV MidiCaps cartridge (Sartorius) with a double membrane of polyethersulfone, and the remainder parts made of

polypropylene (Figure 22). For each UCC CTD bottle the 0.2 µm Sartobran 300 cartridge was firstly rinsed with 700 ml sample to replace the previous sample from the cartridge. The < 0.02 µm Virosart CPV MidiCaps cartridge was first emptied from its previous seawater sample and rinsed with 500 ml of the new sample before a final sample was taken.

Samples for DFe, total dissolvable Fe, and sizefractionated Fe concentrations were acidified within 24 hrs after sampling using ultrapure HCl (pH 1.8, 2ml/L 12M Baseline grade Seastar HC).

Figure 22. Ultrafiltration of seawater samples directly from the UCC CTD bottles.

The samples will be measured using FIA with detection based on luminol chemiluminescence at the home laboratory according to an improved chemiluminescence flow injection method (Klunder et al. 2011). At least 12h prior to analysis, 60 µL of 10 mM H_2O_2 (Suprapure, Merck 30%) will be added to ensure the oxidation of any Fe(II) in the sample (Lohan and Bruland, 2006). The acidified sample will be pre-concentrated for 120 s on a Toyopearl AF-Chelate-650M (TosoHaas, Germany) column. Hereafter the column will be rinsed for 60 s with MQ water to remove interfering salts. The Fe was subsequently eluted from the column with 0.4 M HCl (Suprapure, Merck 30%) during 120 s. The eluted Fe/HCl mixture subsequently mixes with a 0.96 M ammonium hydroxide (Suprapur, 25% Merck), 0.3M hydrogen peroxide (Suprapure, Merck 30%) and luminol/TETA solution (3 ml luminol stock solution and 60 µL TETA 1 L ultrapure water). The luminal stock solution will be prepared by dissolving 270 mg luminol (3-aminophtal-hydrazide, Aldrich) and 500 mg potassiumhydroxide in 15 ml ultra pure type 1 water (18.2 MΩ). Sample and reaction solution will pass a 1.5 m length mixing coil placed in a 35°C water bath. The chemiluminescence will be detected with a Hamamatsu HC135 Photon counter. Concentrations of dissolved Fe will be calculated in nanomol/liter (nM) from the photon emission peak height.

The system will be calibrated using standard additions from a 895 nM Fe stock solution (Fluka) to filtered acidified seawater of low Fe concentration that was collected in the sampling area. A five-point calibration and blank determination will be made daily. The blank will be determined as the intercept of the signals of increasing pre-concentration times (5, 10,

15 seconds) of the calibration water. A certified SAFe standard (Johnson et al. 2007) for the long term consistency and absolute accuracy will be measured on a regular basis.

References

De Baar, H.J.W., K.R. Timmermans, P. Laan , H.H. De Porto, S. Ober, J.J. Blom, M.C. Bakker, J. Schilling,G. Sarthou, M.G. Smit and M. Klunder (2008) Titan: A new facility for ultraclean sampling of trace elements and isotopes in the deep oceans in the international Geotraces program, Marine Chemistry, 2008.

Johnson et al., 2007. Developing standards for dissolved iron in Seawater. Eos, Vol 88, n. 11.

Klunder, M. B., P. Laan, R. Middag, H. J. W. De Baar, and J. C. van Ooijen (2011), Dissolved iron in the Southern Ocean (Atlantic sector), *Deep Sea Research Part II: Topical Studies in Oceanography*, *58*(25-26), 2678-2694

Lohan, M.C. and Bruland, K.W., 2006. Importance of vertical mixing for additional sources of nitrate and iron to surface waters of the Columbia River plume: Implications for biology. Mar. Chem., 98: 260-273

Martin, J. H., and R. Michael Gordon (1988), Northeast Pacific iron distributions in relation to phytoplankton productivity, *Deep Sea Research Part A. Oceanographic Research Papers*, 680 *35*(2), 177-196.

4.2.A.2. Organic speciation of Fe

Micha Rijkenberg[1] for Loes Gerringa[1] and Stan van den Berg[2]

[1]Royal Netherlands Institute for Sea Research, Texel, the Netherlands
[2]University of Liverpool, UK

Introduction

Fe is an interesting element in the ocean and has been studied intensively because it is essential micronutrient for phytoplankton growth and the concentrations in seawater are extremely low. High Nutrient Low Chlorophyll (HNLC) regions in the oceans can partly be explained by a lack of Fe (de Baar et al, 1990, 1995; Johnson et al, 1997). Outside the HNLC regions Fe apparently is not limiting but still present in relatively low concentrations. The concentrations of Fe are so very low in seawater because the solubility product of the oxy-hydroxides of Fe is very low at the pH and oxygen concentrations of normal seawater (Liu and Millero, 2002). However, the dissolved Fe concentrations below the photic zone are higher than predicted by this solubility product. Since 1994 it is known that around 99% of dissolved Fe in seawater is bound to organic molecules that bind Fe very strongly (Gledhill and van den Berg, 1994). This so called organic complexation is important because it increases the solubility of Fe in seawater and enables concentrations above the solubility product. The binding by dissolved organic molecules, called ligands, prevents or at least retards precipitation of Fe as insoluble oxides. Organic complexation also influences the bioavailability of Fe. Part of the complexed Fe must be taken up by phytoplankton, although it is not quite clear how (Shaked et al., 2005, Salmon et al., 2006).

During this cruise <0.2 µm filtered seawater samples were taken from the full depth casts (station 3-7) as well as from the shallow casts in order to investigate its fine distribution in the upper layer of the water column (280 m, stations 3-12).

Samples were also taken for Van den Berg to measure among others humic Fe binding

material. These substances originating from soils enter the ocean by rivers. Results will show if humic Fe binding substances exists in the open ocean and what their contribution is to the dissolved organic ligands pool (Laghlera et al. 2011).

Methods

Seawater (< 0.2 µm) was sampled as described in section 4.2.A.1. The samples were not acidified but immediately frozen and stored at -20°C. The samples will be analyzed in the NIOZ home laboratory. At station 4 all depths were sampled with 1 L samples for Loes Gerringa and 500 ml samples for Stan van den Berg. This to provide an intercomparison between both labs.

Analysis

At NIOZ and by Loes Gerringa, the natural ligand characteristics will be determined by doing a complexing ligand titration with addition of iron (between 0 and 8 nM of Fe added) in buffered seawater (mixed NH_3/NH_4OH borate buffer, 5 mM). The competing ligand 'TAC' (2-(2-Thiazolylazo)-p-cresol) with a final concentration of 10 µM will be used and the complex $(TAC)_2$-Fe will be measured after equilibration (> 6 h) by cathodic stripping voltammetry (CSV) (Croot and Johansson, 2000). The electrical signal recorded with this method (nA) will be converted as a concentration (nM), then the ligand concentration and the binding strength will be estimated using the non-linear regression of the Langmuir isotherm (Gerringa and al., 1995).

The voltammetric equipment consists of a µAutolab potentiostat (Type II, Ecochemie, The Netherlands), a mercury drop electrode (model VA 663 from Metrohm) and a sample changer. All equipment is protected against electrical noise by a current filter (Fortress 750, Best Power).

Stan van den Berg will measure the same samples using the same method of CSV, but with a different competing ligand: DHN (van den Berg, 2006) and the presence of humic Fe binding material using CSV (Laglera and van den Berg, 2009).

References

Croot P.L., Johanson M., 2000. Determination of iron speciation by cathodic stripping voltammetry in seawater using the competing ligand 2-(2-Thiazolylazo)-p-cresol (TAC). Electroanalysis. 12, No.8, 565-576.

de Baar, H.J.W., Buma, A.G.J., Nolting, R.F., Cadee, G.C., Jacques, G., Tréguer, P.J., 1990. On iron limitation of the Southern Ocean: experimental observations in the Weddell and Scotia Seas. Mar. Ecol. Progress Ser. 65, 105–122.

de Baar, H.J.W., de Jong, J.T.M., Bakker, D.C.E., Löscher, B.M., Veth, C., Bathmann, U., Smetacek, V., 1995. Importance of iron for phytoplankton spring blooms and CO2 drawdown in the Southern Ocean. Nature 373, 412–415.

Gerringa, L.J.A., Herman, P.M.J., Poortvliet, T.C.W., 1995. Comparison of the linear Van den Berg/Ruzic transformation and a non-linear fit of the Langmuir isotherm applied to Cu speciation data in the estuarine environment. Mar. Chem., 48, 131-142.

Gledhill, M. and van den Berg, C.M.G., 1994. Determination of complexation of iron (III) with natural organic complexing ligands in seawater using cathodic stripping voltammetry. Mar. Chem., 47: 41-54.

Johnson, K.S., R. M Gordon, K. H. Coale, 1997. What controls dissolved iron concentrations in the world ocean? Marine Chemistry 57, 137-161

Laglera, L.M. and van den Berg, C.M.G., 2009. Evidence for geochemical control of iron by humic substances in seawater. Limnol. Oceanogr., 54(2): 610-619.
Laglera, L.M., Battaglia, G. and van den Berg, C.M.G., 2011. Effect of humic substances on the iron speciation in natural waters by CLE/CSV. Marine Chemistry, 127: 134-143.
Liu, X., Millero, F.J., 2002. The solubility of iron in seawater. Mar. Chem. 77, 43-54.
Shaked, Y., Kustka, A.B., Morel, F.M.M., 2005. A general kinetic model for iron acquisition by eukaryotic phytoplankton. Limnol. Oceanogr. 50: 872–882.
Salmon, T.P., Andrew L. Rose, A.L., Neilan, B.A., Waite, T.D., 2006. The FeL model of iron acquisition: Non-dissociative reduction of ferric complexes in the marine environment. Limnol. Oceanogr., 51, 1744–1754
van den Berg, C.M.G., 2006. Chemical speciation of iron in seawater by cathodic stripping voltammetry with dihydroxynaphthalene. Analytical Chemistry, 78(1): 156-163.

4.2.A.3. The biogeochemical cycles of cobalt, zinc and cadmium in the western North Atlantic Ocean

Gabriel Dulaquais

Institut Universitaire Européen de la Mer (UBO), Brest, FRANCE
LEMAR UMR 6539 (UBO/CNRS/IRD)

1. Introduction

Unprecedented efforts are conducted worldwide to map the distribution of trace elements and isotopes in the context of the international GEOTRACES program in the global oceans. Cobalt (Co), zinc (Zn) and cadmium (Cd) are key trace metals highlighted in the GEOTRACES Science Plan. They are essential micronutrients, driving the productivity and spatial distribution of specific taxa (Sunda and Huntsman, 1995; Saito *et al.,* 2002; Jakuba *et al.,* 2008).

The internal cycles of Zn and Cd are nutrient-like and follow two nutrient distributions, Zn follows silicic acid (Lohan *et al*., 2002; Bruland, 1980; Martin *et al*., 1990; Ellwood, 2008) and Cd follows the phosphate distribution (de Baar et al., 1994; Saager et al., 1997; Ellwood, 2008). By contrast the behavior of Co has been described as a hybrid type metal, as for iron, a nutrient-type behavior is observed in the surface ocean and a scavenging type of behavior in the deep ocean. Despite the correlation between Co and phosphate in the surface ocean as described in several studies (Martin et al., 1989; Saito and Moffett, 2002; Saito *et al., 2004; 2010;* Jakuba et al., 2008; Noble et al., 2008; Bown *et al*., 2011) the low solubility of Co and its scavenging by particles prevent its accumulation in deep waters of the Pacific along the thermohaline circulation through the deep basins. Furthermore, the competition between Co scavenging and its stabilization in solution by the complexation with organic binding ligands seem to be the two major processes controlling the Co cycle in the deep ocean (Saito et al, 2002). In surface waters, the organic complexation of cobalt prevents its scavenging, increases its bioavailability and slows down its removal by microbial co-oxidation with manganese (Bown et al., 2012). Co often co-varies with Mn, but their abiotic removal pathway is in competition with its biological assimilation in surface waters which can lead to a decoupling between the cycles of Co and Mn (Moffett and Ho, 1996). In the

oligotrophic central Atlantic, the cobalt uptake relative to phosphate uptake is more than an order of magnitude higher than in the surface northeast Pacific, whereas zinc uptake relative to phosphate uptake is similar in both areas (Martin and Gordon, 1988; Martin *et al.*, 1989, Saito et al., 2002). It implies that Co is relatively more biologically important than Zn in the oligotrophic Atlantic (Saito and Moffett, 2002). It suggests therefore that the biogeochemical cycle of Co and Mn was decoupled in the oligotrophic Atlantic Ocean. Furthermore, the geochemical cycles of Co, Zn, and Cd have shown to be connected in the surface waters through biochemical cambialistic substitutions in the alkaline phosphatase and the carbonic anhydrase complexes (Roberts *et al*., 1997; Lane *et al*., 2005; Saito *et al*., 2008). These observations, lead us to hypothesize that the Co:P ratios can be controlled by the concentrations and the biological requirement for Zn and Cd of specific taxa in the oligotrophic central Atlantic Ocean. Finally, the Cd uptake by phytoplankton and the particulate Cd:P ratios can both increase under Zn depletion or Fe limitation (Sunda and Huntsman, 2000; Cullen *et al*., 2006; Lane *et al*., 2008) implying a coupling between the cycles of these three metals.

External sources of Co, Zn and Cd to the ocean form an integral part of their marine biogeochemical cycling. Hydrothermal sources, dust and river inputs but also diffusion in or out of sediments or sediment resuspension can be sources or sinks for these metals depending on their oxidation state and/or conditions. Interactions with atmospheric particles can release or remove metals from the surface ocean. In fact, due to the relatively low pH of rainwater, and the strong pH dependence of transition metal solubility (Stumm and Morgan, 1996), wet deposition may constitute a major source of trace metals to the open ocean (Helmers and Screms, 1995; Jickells, 1999; Baker et al. 2007, Shelley et al., 2012). By contrast adsorption of metals to particles that enter the ocean with dry deposition seems to be a pathway to export metals from the upper to the deep ocean (Thuróczy et al., 2010). Biotic particles are also exporting metals from the surface waters to the deep ocean but the remineralization and possibly the desorption may release metals in deeper waters. The transportation from continental shelf and slope waters towards the open ocean can be another external source in intermediate and deep waters (Noble et al., 2008), like recently evidenced for Co in the southeastern Atlantic Ocean (Bown et al., 2011).

The aim of this study is to complete the previous NL-A02 GEOTRACES section which has been sampled in three legs from 64°N to 50°S in the West Atlantic Ocean to describe the distribution and physico-chemical speciation of Co, Zn and Cd. Here 5 new deep stations completed leg 1 (64PE319). Five additional shallow stations (down to 280 m depth) were sampled along the northern branch of the Gulf Stream. We sampled for dissolved and total dissolvable Co, Zn and Cd and for the organic speciation of Co like we did during the 3 first legs. In addition, we took size-fractionated samples to distinguish between the truly soluble and colloidal fraction of dissolved Co, Zn and Cd. Size fractionation will allow us to investigate the internal processes of these metals and their interaction with the biota in the surface waters. It will also reveal if size fractionation occurs during remineralization and scavenging processes in deeper waters. Meridional gradient of the oxygen concentrations has been observed along the A02-section and this will be studied in relation to changes in the size fractionation of those three metals. Finally concentrations will be determined along the northern branch of the Gulf Stream (Figure 22); this will reveal Co, Zn and Cd dynamics over zonal transportation in the surface North Atlantic.

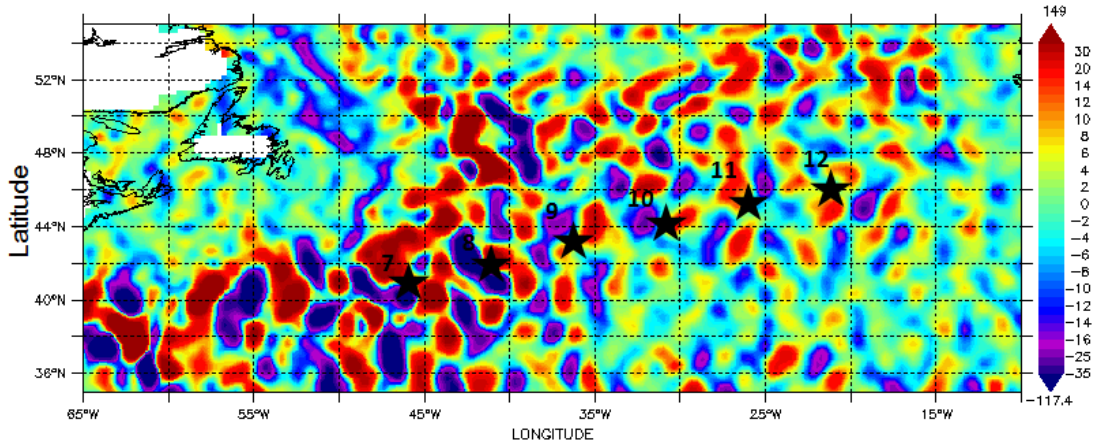

Figure 22. East component of the zonal geostrophic velocity in cm/s (7 August 2012). The figure shows the barotropic component of the geostrophic current, resulting from the altimetry data. The positive values (red) indicate a current from the west to the east and the negative values indicate a current from the east to the west. Stations 7 to 12 are plotted (dark stars). Source: http://las.aviso.oceanobs.com

2. Methods

Sampling of trace metals

Cobalt, zinc and cadmium were sampled using the ultraclean sampling facilities of NIOZ specifically developed for trace metal sampling. The ultraclean CTD (UCC) contains 24 large volume (27 L) samplers made of PVDF on a titanium frame with sensors for conductivity, temperature, pressure, oxygen, light transmission (inverse for particles abundance). For sampling, the UCC is immediately placed in a clean air container after recovery. A total of 10 stations were sampled (station 3 to 12) with two hydrocasts (deep and shallow) sampled on the first five stations and one shallow hydrocast sampled on the last five stations.

Deep cast

Filtered (0.2µm) samples to determine dissolved metals concentrations and the organic speciation of cobalt were sampled at the 5 deep hydrocasts achieved along the section from Reykjavik to station 7. Unfiltered samples were also collected to estimate apparent particulate metals concentrations (as the difference between unfiltered and filtered fractions). Ultrafiltered (< 0.02µm) samples were collected at two depths (oxygen minimum and bottom depth). During the downcast of the CTD, parameters as density, oxygen concentration and fluorescence were used to determine the sampling strategy and optimize the resolution at depth. The vertical resolution is reported in Table 2.

Shallow cast

Filtered and ultrafiltered samples were collected at 8 depths of the 10 shallow hydrocasts. As for deep hydrocasts CTD parameters were used to optimize the resolution (Table 2).

Table 2. Water column samples taken from the UCC CTD. In blue the two bottles collected for ultrafiltration on the Deep casts (D), at Shallow cast (S) ultrafiltration samples have been collected for each bottle. Parameters: Dissolved samples (D), Unfiltered samples (T), Ultrafiltered samples (SF), Co-organic speciation samples (CoL).

Station	Cast / Type	Bottles n°	Parameters
3	1/D	1,2,3,5,8,10,12,13,14,17,18,19,20,21,23,24	D, T, CoL
3	2/S	5,13,15,18,20,21,23,24	D, SF
4	1/D	**1**,2,3,5,7,**9**,11,12,13,15,17,18,19,21,22,23,24	D, T, **SF**, CoL
4	2/S	5,10,15,17,29,21,23,24	D, SF
5	1/D	**1**,2,4,5,6,9,11,12,13,15,**16**,19,20,21,22,23,24	D, T, **SF**, CoL
5	2/S	4,5,10,18,19,20,21,23	D, SF
6	1/D	**1**,3,4,6,8,10,12,**13**,14,16,18,19,20,21,23,24	D, T, **SF**, CoL
6	2/S	3,5,6,13,17,18,22,24	D, SF
7	1/D	**1**,3,4,6,8,12,**13**,14,16,18,19,20,21,22,24	D, T, **SF**, CoL
7	2/S	3,5,6,13,17,18,20,24	D, SF
8	1/S	5,8,12,15,16,17,20,24	D, SF
9	1/S	5,8,12,15,16,18,20,24	D, SF
10	1/S	5,8,9,13,17,18,22,24	D, SF
11	1/S	1,4,9,13,17,18,20,24	D, SF
12	1/S	1,3,8,13,17,19,21,24	D, SF

Analyses of dissolved, ultra-filtered, total and the organic speciation of cobalt

At the home laboratory dissolved, total and ultrafiltered concentrations of cobalt will be measured in acidified (pH~1.9-2) and UV-digested samples by FIA-Chemiluminescence method with toyopearl preconcentrating column and acidified ammonium acetate (pH 4) as a column conditioning step prior to the sample loading and the rinse steps, following the method adapted from Shelley et al., 2010 (Bown et al., 2011). Concentrations are estimated by two daily calibrations made at the start and the end of a series of samples. The accuracy of the method was evaluated by determining dissolved cobalt in acidified North Pacific deep and surface seawater samples from the Sampling and Analysis of Iron (SAFe) program. The method yields mean values of 4.76 ± 1 pM in surface (S) and 45.21 ± 2.6 pM in deep (D2) (Dulaquais et al., in prep.), which is in excellent agreement with the SAFe consensus values of 5.4 ± 2.2 pM and 45.4 ± 3.8 pM, surface and deep reference waters respectively. The organic speciation of Co will be measured at the home lab in filtered (0.2 µm) and frozen-stored samples (-20°C) by Cathodic Stripping Voltammetry (Ellwood *et al.* 2001; 2005).

Analyses of dissolved, ultra-filtered and total zinc and cadmium

Total, dissolved and ultrafiltered zinc and cadmium will be measured simultaneously in unfiltered, filtered (0.2 microm) and in ultrafiltered (0.02µm) acidified samples (pH~1.8) by voltammetric method (adapted from: Ellwood and van den Berg, 2000, Jakuba *et al*., 2008 for Zn; and Bruland, 1992, Ellwood, 2004 for Cd). Successful analyses using these adapted methods were achieved in samples collected during the previous NL-A02 GEOTRACES cruises at the home-lab (Dulaquais et al., in prep.). Dissolved zinc and cadmium will be analyzed in the acidified samples without any added reagents using HMDE Anodic Stripping Voltammetry. Square wave is used with a scan rate of 148.5 mV, using a deposition potential of -1.4 V during 180 to 1200 sec, a frequency of 30 Hz, and a scan in potential between -1.35 V and -0.35 V. Zinc is detected at the potential of -0.987 V and Cd at -0.573 V. The concentrations of Zn and Cd are calibrated against 2 standard additions of a bi-elementary

solution. Concentrations added in the sample and deposition time depend of the depth of sampling. As for Co analyses, the accuracy of the method was evaluated by determining dissolved Zn and Cd in acidified North Pacific deep and surface seawater samples from the Sampling and Analysis of Iron (SAFe) program. The method yields mean 7.05 ±0.3 nM and 963 ± 11pM respectively for Zn and Cd in deep (D2) which is also in excellent agreement with the SAFe consensus values of 7.2 ± 0.5 nM and 986 ± 27 pM deep reference waters for Zn and Cd, respectively (Dulaquais et al., in prep.).

3. Observations

During the cruise, 2 major events have to be headlined. **(1)** During the sampling of station 5 due to the time used to collect samples, the shallow hydrocast has been done during the night unlike the deep hydrocast (sampled during the day). Between these two casts, physical parameters did not change unlike the fluorescence profile. During the day the fluorescence profile is more stratified than during the night. This variation is most likely due to the migration of the biota. Several studies have shown that the zooplankton moves with the light incidence (Bollens & Frost, 1989; Landry et al., 2001; Hannides et al., 2009). The zooplankton rises to the surface during the night and is in majority in the unfiltered fraction (>0.2µm). Cellular quotas in traces metals vary with the plankton taxa, implying that any potential variations of trace metals detected in the different fractions at a same depth between the two casts in the first 100 meters layer will reveal zooplancton migration. **(2)** Submesoscale eddies were detected three weeks before sampling at the latitudes of stations 6 and 7 by altimetry data (Aviso.obs). Based on the evolution of the eddies over 1 month before sampling (Figure 23), station 6 was probably located inside an eddy, whereas station 7 was outside. Submescoscale eddies are known to move the density and nutrients isolines (McWilliams, 1991). Furthermore the eddy dynamic can fertilize the biota in nutrients by vertical injection into filaments and also by lateral advection into its core, with co-existing different phytoplanktonic populations (Abraham. 1998; Lapeyre & Klein. 2006). Such mesoscale eddies can also influence the distributions of Co, Zn and Cd, with potentially significant differences between these two stations despite their close location, and implication for the growth and cellular metals quota of the taxa,. For example an accumulation of Co in the upper water and shift in the Co:P ratio can be caused by a cyclonic eddy (Noble et al., 2008).

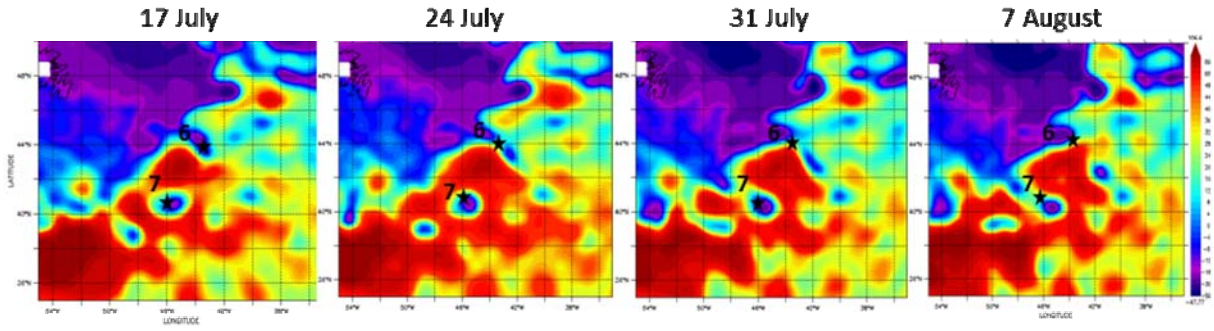

Figure 23. Time evolution of the absolute dynamic topography (in cm) in the area of stations 6 and 7 one month before their sampling. Station 6 and 7 are plotted (dark stars). Source: http://las.aviso.oceanobs.com

4. Investigating the potential impact of volcanic eruption

In May 2010, a few weeks after the volcanic eruption of an Icelandic volcano (Eyjafjallajökull), LEG-1 of the G0A2-section has been sampled in the North West Atlantic Ocean. Because a cloud of volcanic ash was reported to cover most of the East Atlantic and Europe during 64PE319, a comparison between the two cruises of the subsurface metal concentrations in the northern section will be interesting. In fact, a linear southward decrease ($R^2 > 0.96$) of surface DCo concentrations was observed during LEG-1 from 64°N to 37°S (Figure 24). Co analyzes in subsurface water at station 3 ,4, 5, 6 and 7 may help us to understand if this strong gradient is due to an episodic Co source linked to the volcano eruption in the North of the section or if it should be integrated as a biogeochemical features of the Co cycle in the North Atlantic.

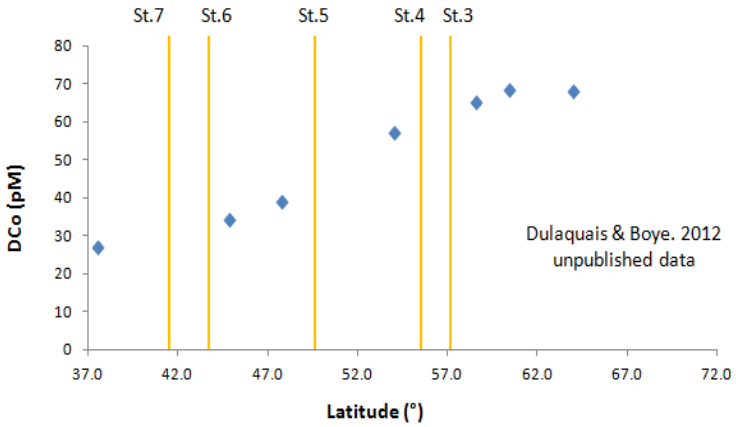

Figure 24. Meridional distribution of dissolved Co in subsurface waters (25 m) in the North West Atlantic Ocean during LEG-1 (02-18 May 2010). A latitudinal linear decrease is observed from the North to the South with a strong correlation between 64° N and 37° N (R^2>0.959; n=8). Yellow bars indicate the location of the 5 stations completing the GEOTRACES NL-A02 section. Unpublished data from Dulaquais & Boye 2012.

Acknowledgments

We thank the Captain and crew of the R.V. Pelagia, Micha Rijkenberg as chief scientist of the cruise, Sven Ober and Jack Underwood for CTD data, Sharyn Crayford for nutrients data, Nikki Clargo for Alkalinity Data, Sophie Vergouwen and Audrey van Mastrigt for collecting samples. The PhD research of G.D. is supported by a COST-ES0801 grant, UBO and Region Bretagne, and by a research project financed by INSU-CNRS (PI M. Boye).

References

Abraham E.R. 1998 The generation of plankton patchiness by turbulent stirring, Nature, 391, 577-580

Baker, A.R.et al, 2007, Dry and wet deposition of nutrients from the tropical Atlantic atmosphere: Links to primary productivity and nitrogen fixation. Deep Sea Res. Part I, 54, 1704-1720.

Bollens S.M. & Frost B.W. 1989 Predator-induced diet vertical migration in a planktonic copepod Oxford Journals. Life Sciences. Journal of Plankton Research. Volume 11, Issue 5 Pp. 1047-1065.

Bowie A. R. et al., 2002 Biogeochemistry of Fe and other trace elements (Al, Co, Ni) in the upper Atlantic Ocean, *Deep Sea Res*. 49, 605-636

Bown J., M. Boye, A. Baker, E. Duvieilbourg, F. Lacan, F. Le Moigne, F. Planchon, S. Speich, D.M. Nelson., 2011 The biogeochemical cycle of dissolved cobalt in the Atlantic and the Southern Ocean south off the coast of South Africa. Marine Chemistry, 126, 193-206

Bruland, K.W., 1980. Oceanographic distributions of cadmium, zinc, nickel and copper in the

North Pacific, Earth Planet. Sci. Lett., 47, 176–198.
Bruland, K.W., 1992. Complexation of cadmium by natural organic ligands in the central North Pacific. Limnol. Oceanogr. 37, 1008-1017.
Cullen, J. T., 2006. On the nonlinear relationship between dissolved cadmium and phosphate in the modern global ocean: could chronic iron limitation of phytoplankton growth cause the kink? Limnol. Oceanogr., 51, 1369–1380.
de Baar, H. J. W., Saager, P. M., Nolting, R. F., and van der Meer, J, 1994.: Cadmium versus phosphate in the world ocean, Mar. Chem., 46, 261–281.
Ellwood, M.J., 2004. Zinc and cadmium speciation in subantarctic waters east of New Zealand. Marine Chemistry 87, 37-58.
Ellwood, M.J., C.M.G. van den Berg, 2000. Zinc speciation in the northeastern Atlantic Ocean, Mar. Chem., 68, 295– 306.
Ellwood and van den Berg, 2001. Determination of organic complexation of cobalt in seawater by cathodic stripping voltammetry. *Marine Chemistry*, 75, 33-47.
Ellwood, van den Berg, Boye *et al.*, 2005. Organic complexation of cobalt across the Antarctic polar front in the Southern Ocean. *Marine and Freshwater Research*, 56, 1069-1075.
Ellwood, 2008. Wintertime trace metals (Zn, Cu, Ni, Cd, Pb and Co) and nutrient distributions in the Subantarctic Zone between 40-52°S; 155-160°E. Marine Chemistry, 112(1-2): 107-117.
Fitzwater S. E. et al, 2000 Trace metal concentrations in the Ross Sea and their relationship with nutrients and phytoplankton growth. *Deep Sea Res*. 47, 3159-3179
Hannides C.C.S. et al, 2009 Quantification of zooplankton trophic position in the North Pacific Subtropical Gyre using stable nitrogen isotopes. Limnology and oceanography, 54, 60-61
Helmers, E. and O. Schrems 1995, Wet deposition of metals to the tropical North and the South Atlantic Ocean. Atmos. Env., 29, 2475-2484.
Jakuba, R.W., Moffett, J.W. and 860 Dyhrman, S.T., 2008. Evidence for the linked biogeochemical cycling of zinc, cobalt, and phosphorus in the western North Atlantic Ocean. Global Biogeochemical Cycles, 22(4).
Jickells, T. 1999, The inputs of dust derived elements to the Sargasso Sea; a synthesis, Mar. Chem., 68, 5-14.
Kremling, K., Streu, P. 2001 The behaviour of dissolved Cd, Co, Zn, and Pb in North Atlantic near-surface waters (301N/601W–601N/21W), *Deep Sea Res.* 48, 2541-2567
Landry M.R. et al, 2001 Seasonal patterns of mesozooplankton abundance and biomass at Station ALOHA, *Deep Sea Res*. 48, 2037–2061
Lane, T. W., Saito, M. A., George, G. N., Pickering, I. J., Prince, R. C., and Morel, F. M. M., 2005. A cadmium enzyme from a marine diatom, Nature, 435, 42,.
Lane, E. S., Jang, K., Cullen, J. T., and Maldonado, M. T., 2008. The interaction between inorganic iron and cadmium uptake in the marine diatom *Thalassiosira oceanica*, Limnol. Oceanogr., 53, 1784–1789.
Lapeyre G. and Klein P. 2006, Dynamics of the Upper Oceanic Layers in Terms of Surface Quasigeostrophy Theory, Journal of Physical Oceanography, 36, 165-172
Lohan M.C., Statham P.J. and Crawford D.W., 2002. Total dissolved zinc in the upper water column of the subarctic North East Pacific. Deep Sea Res. II 49, 5793-5808.
Martin and Gordon, 1988. Northeast Pacific iron distribution in relation to phytoplankton productivity. *Deep-Sea Res.* 35, 177–196.

Martin *et al*., 1989. VERTEX: Phytoplankton/iron studies in the Gulf of Alaska. *Deep-Sea Res.* 36, 649 – 680.

Martin J.H., 1990. Glacial-interglacial CO_2 change: the iron hypothesis. *Paleoceanography*, 5: 1-13.

Noble et al., 2008; Cobalt, manganese, and iron near the Hawaiian Islands: A potential concentrating mechanism for cobalt within a cyclonic eddy and implications for the hybrid type-trace metals. *Deep Sea Res*. 55, 1473-1490

McWilliams, J. C. 1985; Submesoscale, Coherent Vortices in the Ocean, Rev. of Geoph. 23. 2 165-182.

McWilliams, J. C. 1991; Geostrophic Vortices, *Proceedings of the Summer School ENRICO FERMI.*

Morel, F. M. M. et al, 1991; Limitation of productivity by trace metals in the sea, *Limno. Oceanog.* 36, 1742- 1755.

Moffett and Ho, 1996. Oxidation of cobalt and manganese in seawater via a common microbially catalyzed pathway. *Geochim. Cosmochim. Acta* 60, 3415–3424

Roberts, S., Lane, T., and Morel, F. M. M., 1997. Carbonic anhydrase in the marine diatom *Thalassiosira weissflogii* (*Bacillariophyceae*), J. Phycol., 33, 845–850.

Saager et al., 1997; Saager P.M., H.J.W. de Baar, J.T.M. de Jong, R.F. Nolting, J. Schijf, 1997. Hydrography and local sources of dissolved trace metals Mn, Ni, Cu, and Cd in the northeast Atlantic Ocean. *Marine Chemistry 57, 195-216.*

Saito and Moffett, 2001. Complexation of cobalt by natural organic ligands in the Sargasso Sea as determined by a new high-sensitivity electrochemical cobalt speciation method suitable for open ocean work. *Mar. Chem.* 75, 49 – 68.

Saito and Moffett, 2002. Temporal and spatial variability of cobalt in the Atlantic Ocean. *Geochimica et Cosmochimica Acta*, 66, 1943–1953.

Saito, M.A. and Goepfert, T.J., 2008. Zinc-cobalt colimitation of Phaeocystis antarctica. Limnology and Oceanography, 53(1): 266-275.

Saito, M.A., Goepfert, T.J., Noble, A.E., Bertrand, E.M., Sedwick, P. and DiTullio, G.R., 2010. Seasonal study of dissolved cobalt in the Ross Sea, Antarctica: micronutrient behavior, absence of scavenging, and relationships with Zn, Cd, and P. Biogeosciences Discussion 7, 6387–6439, 2010

Shelley, R.U., Zachhuber, B., Sedwick, P.N., Worsfold, P.J. and Lohan, M.C., 2010. Determination of total dissolved cobalt in UV-irradiated seawater using flow injection with chemiluminescence detection. Limnology and Oceanography: Methods., 8: 352-362.

Shelley, R.U et al., 2012 Controls on dissolved cobalt in surface waters of the Sargasso Sea. *Global Biogeochem. Cycles* submitted.

Stumm W. and Morgan J.J., 1996, Aquatic Chemistry: Chemical Equilibria and Rates in Natural Water. Wiley, Chichester.

Sunda, W.G. and Huntsman, S.A., 1995. Cobalt and zinc interreplacement in marine phytoplankton: Biological and geochemical implications. Limnology and Oceanography, 40(8): 1404-1417.

Sunda, W. G. and Huntsman, S. A., 2000. Effect of Zn, Mn, and Fe on Cd accumulation in phytoplankton: implications for oceanic Cd cycling, Limnol. Oceanogr., 45, 1501–1516.

Thuróczy, C.E., Boye, M. and Losno, R., 2010. Dissolution of cobalt and zinc from natural and anthropogenic dusts in seawater. *Biogeosciences*, 7(6): 1927-1936.

Yeats P. A., S. Westerlund, A. R. Flegal, 1995. Cadmium, copper and nickel distributions at four stations in the eastern central and south Atlantic. *Marine Chemistry*, *49, 283-293*
Yeats P. A., 1998. An isopycnal analysis of cadmium distributions in the Atlantic Ocean. *Marine Chemistry 61, 15-23.*

4.2.B. CO_2 and other transient anthropogenic tracers

4.2.B.1. Dissolved Inorganic Carbon, Total Alkalinity

Nikki Clargo

Royal Netherlands Institute for Sea Research, Texel, the Netherlands

Sampling and analysis for carbonate system parameters broadly followed the standard operating procedures outlined by Dickson et al., 2007.

Water samples of 0.6 L were collected from the Ultra Clean CTD from the first cast of every station, at all 24 depths, into borosilicate sample bottles with plastic caps, using tygon tubing. In each profile, three duplicate samples were collected at shallow, intermediate and deep parts of the cast (with the exception of the shallow cast at station 14, where no intermediate duplicate was taken). Sample analysis commenced immediately after collection. Analysis of surface samples was in all cases completed within 12 hours after sampling. All analyses were performed on a VINDTA 3C (Versatile INstrument for the Determination of Total Alkalinity, designed and built by Dr. L. Mintrop, Marine Analytics and Data, Kiel, Germany) (Figure 25).

Samples were measured simultaneously on two instruments, referred to as A and B (VINDTA #17 and #14, respectively). These instruments were slightly modified: the peristaltic sample pump was replaced with an overpressure system (~0.5 bar overpressure) and a 1m long (though coiled) 1/8" stainless steel counter-flow heat exchanger that was placed between the sampling line and the circulation circuit. This setup allows for the rapid, convenient and bubble-free loading of the pipettes with sample of 25ºC (± 0.1ºC), irrespective of the samples' initial temperature.

Duplicate samples were analyzed first followed by the depth profile beginning with surface samples. This assured that any 'startup drift' in the coulometric cells did not affect the deep samples. The use of two machines increases confidence in final results, and allows demonstration and quantification of measurement errors that would otherwise go unnoticed. No formal analysis and correction of the results have been performed yet. Such a report on the treatment of the carbon data will, in due time, be available as a separate report.

Dissolved inorganic carbon (DIC)
Dissolved inorganic carbon (DIC) was determined by coulometric titration. An automated extraction line takes a 20 mL subsample which is subsequently purged of CO_2 in a stripping chamber containing ~1 mL of ~8.5% phosphoric acid (H_3PO_4). A stream of nitrogen carries the CO_2 gas into a coulometric titration cell via a condenser and acid trap, to strip the gas flow of any water. The CO_2 reacts with the cathode solution in the cell to form

hydroxyethylcarbamic acid, which is then titrated with hydroxide ions (OH^-) generated by the coulometer. The current of the coulometer is then integrated over the duration of the titration to obtain the total amount of carbon titrated.

Total Alkalinity (TA)

Determination of total alkalinity (TA) was performed by acid titration that combines aspects from both the commonly used 'closed cell' method and the 'open cell' method, following VINDTA standard settings. A single 20 L batch of acid of ~0.05M and salinity 35 was prepared to be used by both VINDTAs. Potential drift in acid strength due to HCl-gas loss to acid vessel headspace is not accounted for.

Certified reference material (CRM, Batch #113) obtained from Dr. Andrew Dickson at Scripps Institute of Oceanography (San Diego, California) was used for calibration purposes and quality control for both DIC and TA.

References

Dickson, A.G., Sabine, C.L. and Christian, J.R. (Eds.) 2007. Guide to best practices for ocean CO2 measurements. PICES Special Publication 3, 191 pp.

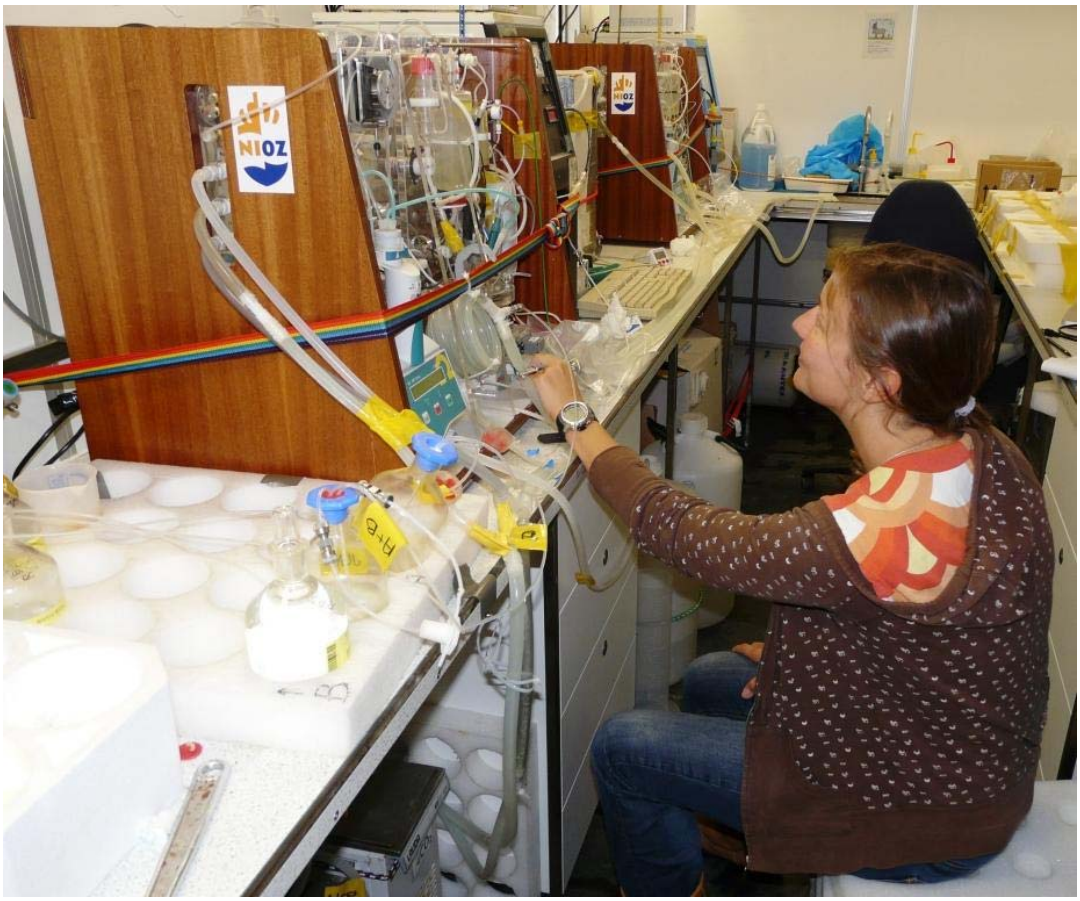

Figure 25. Nikki measures DIC/Alkalinity behind the VINDTA.

4.2.B.2. Isotopes of Dissolved Inorganic Carbon (DIC): $\delta^{13}C$ and $\Delta^{14}C$

Audrey van Mastrigt[1] & Sophie Vergouwen[1],
PI: Steven van Heuven[2]

[1] University of Groningen
[2] Centre for Isotope Research, University of Groningen

Introduction

Samples for determination of the ^{14}C content of the dissolved inorganic carbon were collected for shore based determination of radiocarbon with the use of accelerator mass spectrometry (AMS) at the Centre for Isotope Research (CIO) at the University of Groningen. ^{14}C is an important tracer of various oceanographically relevant processes, such as air-sea gas exchange and abyssal water mass movement and mixing.

In nature, three isotopes of carbon (C) exist: the common, stable ^{12}C (circa 99%), the rare, stable ^{13}C (circa 1%) and the exceptionally rare, unstable 'radiocarbon' ^{14}C (circa $1 \cdot 10^{-10}$ %, $T_{1/2} \approx 5730$ years). The ratios of the concentrations of the isotopes $^{13/12}C$ and $^{14/12}C$ are not exactly constant in place and time, and the deviations from 'normal' (referred to as $\delta^{13}C$ and $\Delta^{14}C$, respectively) are of strong interest to environmental sciences. Determination of these deviations is challenging. For $^{13/12}C$, deviations from 'normal' are caused by isotopic fractionation in physical, chemical and biological processes (and are a measure of the strength of these processes, which is exactly what makes them interesting). Deviations of $^{14/12}C$ are not only the result of the aforementioned fractionation processes, but also of the steady decay of (atmospherically produced) ^{14}C, which becomes noticeable once seawater loses contact with the atmosphere (and thus stops exchanging $^{14}CO_2$). Additionally, anthropogenic changes in the atmospheric composition with respect to ^{13}C and ^{14}C (emissions of low-δC13 CO_2 by combustion of fossil fuels, and the large 'pulse' of ^{14}C produced by atomic bob tests in the 1950s and 1960s, respectively) also imprint on the oceanic values of $\delta^{13}C$ and $\Delta^{14}C$. In the ocean, the cumulative effect of the aforementioned processes on $\delta^{13}C$ is very small: the range of oceanic $\delta^{13}C$ is approximately -1 ‰ to +2 ‰. Determination of $\delta^{13}C$ is only possible by highly precise mass spectrometric analysis. The oceanic range of $\Delta^{14}C$ is much larger (circa -250 ‰ to +150 ‰) but the analysis (by Accelerator Mass Spectrometry; AMS) is nonetheless much more challenging due to the extremely low concentrations of ^{14}C in seawater.

Since the content of ^{14}C of seawater is extremely low and contamination of the samples has occurred on previous cruises, it is of great importance to minimize the possibility of contamination during sampling. A risk of contamination of the samples with non-natural ^{14}C was present during this cruise. This because during the previous cruise (64PE356, MEDEA II), another research team on board conducted ^{14}C-spiking experiments for determination of microbial production.

Methods

Preperation

All work surfaces were cleaned before sampling with hydrochloric acid (0.5 M HCL) and tools were kept in clean zip-lock bags between stations. Sampling lines were kept in a clean bucket filled with 0.1 M HCL solution. A 50% saturated $HgCl_2$ solution was prepared by dissolving 4 g of $HgCl_2$ in 100 ml of MilliQ. Sample bottles were marked with Station-Cast-Bottle-Replicate, and were placed in the Ultraclean container before the UC-CTD came on board.

Sampling

During this cruise, 72 samples were collected on 3 profiles for shore-based determination of carbon isotope ratios at the Centre for Isotope Research (CIO) at the University of Groningen. Sample lines were rinsed before sampling by placing the sampling line in the CTD bottle and open the top and bottom tap for a second or three. At each station, samples were collected from all bottles of the Ultra Clean CTD. Sampling bottles and stoppers were rinsed 3 times before filling. Sample bottles were filled by placing the sampling line at the bottom of the bottle and gradually tapping water while turning the bottle, to let out excess air. Bottles were overflowed twice its volume and 1-2% headspace was kept by removing the sampling line after closure of the tap. Next the stopper was put gently on the bottle and bottles were returned to the lab, where they were poisoned with 125 µL of 50% $HgCl_2$ solution. After poisoning a thin strip of grease was applied to the stopper and the stopper was inserted. Plastic clips were applied to maintain positive closure. After all bottles were poisoned, they were dipped in MilliQ to rinse of salt water, mixed and placed into labelled cartons which were placed in the Zarges box.

Samples were collected at station 4, 5 and 6 from all bottles of the Ultra Clean CTD. The maximum depth and minimum depth were sampled in duplicate.

Remark

At station 5, bottle 5-1-14-a was missing therefore an unlabelled bottle was used.

4.2.C. Microbial oceanography

4.2.C.1. Photo acclimation of Phytoplankton

Audrey van Mastrigt & Sophie Vergouwen

University of Groningen

Introduction

In the water column phytoplankton at different depths are exposed to different light intensities. Due to mixing of the water column phytoplankton can be exposed to light intensities that they might not be acclimated to. On this cruise samples were taken to determine the photo acclimation state of phytoplankton at two different depths, the chlorophyll-a maximum and 10 m below the surface. Photo acclimation of phytoplankton was investigated by determining their photosynthetic efficiency and chlorophyll-a specific absorption in relation to differences in vertical phytoplankton abundance and taxonomic composition.

First of all, the photosynthetic efficiency at different light intensities was determined by making photosynthesis versus irradiance (PI) curves using Fv/Fm as a measure for photosynthetic efficiency (Figure 26). Ten samples were taken from sample bottles from two different depths and exposed to different light intensities ranging from 16 µEin/s to 517 µEin/s. With this information Electron transport Rates (ETR) can be determined which in turn can say something about the productivity of the phytoplankton. ETR is a measure for the number of electrons that are taken up by the photosystem II. By measuring the ETR it the amount of electrons needed for ATP production can be determined and thus the rate of CO_2

fixation during photosynthesis can be determined. Using light filters to create different light intensities, CO_2 fixation rates can be determined per phytoplankton community at different light intensities.

Second, at two depths samples were taken for chlorophyll-a specific absorption and pigment composition. These samples will be analyzed at the University of Groningen, in order to make a comparison between the vertical difference in phytoplankton abundance and phytoplankton taxonomic composition. Phytoplankton abundance will be determined on shore by analyzing chlorophyll-a and doing high-performance liquid chromatography (HPLC). Phytoplankton taxonomic composition will be on shore determined by doing HPLC and looking at pigment composition.

Methods photosynthetic efficiency

One-liter samples were taken from the second shallow cast at two depths, the cholorphyll-a maximum (which varied per station) and at 10 meters depth. Once samples were taken they were quickly stowed away in a black bag to keep them from direct sunlight. At the stations 3-5 ice was added to this bag to keep the samples cool and avoid a heat shock. Before sampling the water temperature was adjusted in the water bath according to the surface water temperature, which was taken from the ships monitor. At the same time the lamp was switched on to heat up and stabilize for 10-15 minutes.

Before starting the experiment the PAM settings were adjusted accordingly (PM gain between 1-30 and PM outgain between 2-5), to achieve a fluorescence (F0) of 300-500 fluorescence units, using a test sample (approximately 30 ml from each liter bottle was used for this). Then the PAM was zeroed with 0.2 µm filtered sea water. Once the settings were correctly adjusted they were kept constant during the PI curves of one depth.

For the chlorophyll-a max as well as the sample taken from 10 m depth we first determined the response of the dark adapted phytoplankton community using 3 x 30 ml of a sample. Next 10 samples (40 ml) were exposed for 20 minutes each to a different light intensity. After 20 minutes the photosynthetic parameters were measured for each sample using the PAM. The resulting PI curves were saved and stored under file name: station-cast-bottle.pam.

During the stations 3-7 the protocol was adjusted slightly because of a misunderstanding. Instead of exposing each sample to exactly 20 minutes of light a time series was performed keeping 1 minute of light exposure between each sample. Thus sample one was exposed to 20 minutes of light, sample 2 to 21 minutes of light, sample 3 to 22 minutes of light etc. up to 30 minutes of light exposure. Maybe the yields can be corrected for the time of exposure.

Methods HPLC and Chl-a filtering

At all possible stations (stations 3-14), two depths per station were sampled based on Chl-a fluorescence sensor from the CTD (chlorophyll maximum), and 10 m below surface. From each depth 10 L for pigment composition (HPLC) and 10 L for Chl-a specific absorption was sampled from the UC-CTD in jerry cans.

A filtration set up was prepared at the wet lab which would apply a maximum of 0.3 bar vacuum. All samples were filtered over 47 mm GF/F filters. Filtered volumes varied between 8 and 10 L, based on pace of filtration. A forceps was used to remove the filter. Filters were wrapped in aluminum foil, labeled with Station-Cast-Bottle. Filters for HPLC were folded, filters for Chl-a specific absorption were not folded. All filters were stored at -80°C. Between stations the filter set-up was rinsed with MilliQ.

Preliminary results

The preliminary results show a trend where the deeper chlorophyll-a max samples had a lower yield compared to the samples taken at 10 meters depth (Figure 26 & 27).

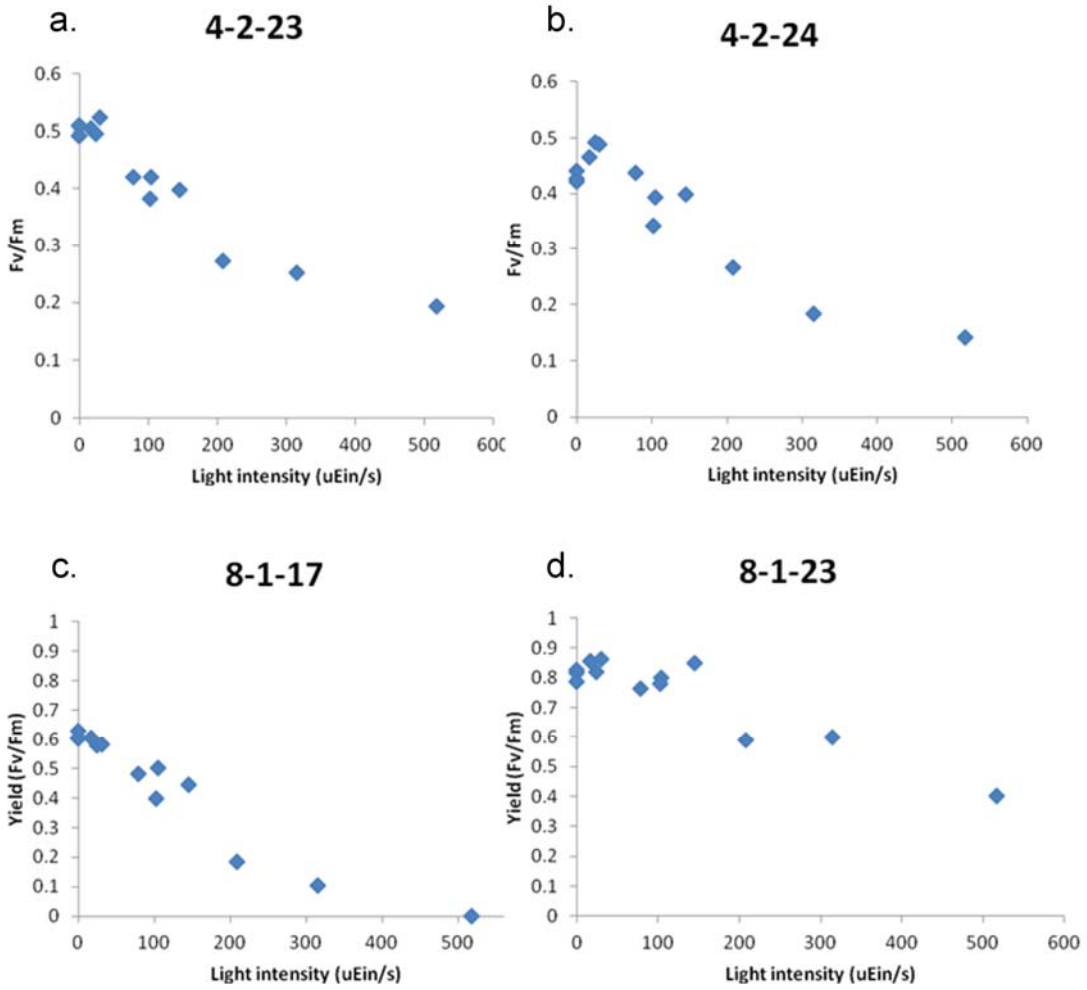

Figure 26. Preliminary results of photo efficiency versus light intensity (PI) curves for a) the Chl a maximum at station 4 cast 2 bottle 23, b) 10 m depth at station 4 cast 2 bottle 24, c) the Chl a max at station 8 cats 1 bottle 17, and d) 10 m depth at station 8 cast 1 bottle 23.

a. b.

Figure 27. a) Sophie filters samples for pigments and Chl-a specific absorption, and b) Audrey uses the PAM to determine the photosynthetic efficiency of the phytoplankton community.

Appendix 1.

Address list of scientist involved in data collection and analysis

Abouchami, Wafa: wafa.abouchami@mpic.de
Max-Planck-Institute for Chemistry
Biogeochemistry dept.
Postfach 3060
55020 Mainz
Germany
Phone: +49 6131 30 52 60
Fax: +49 6131 37 10 51

Achterberg, Eric: eric@noc.soton.ac.uk
Marine Biogeochemistry; School of Ocean & Earth Science
National Oceanography Centre Southampton; University of Southampton
Southampton SO14 3ZH
United Kingdom
Phone direct: 02380-593199
Phone secretary: 02380-592011
Fax: 02380-593059

Hendrik van Aken: Hendrik.van.Aken@nioz.nl
Royal Netherlands Institute for Sea Research
Physical Oceanography
PO Box 59 1790 AB Den Burg
The Netherlands
Phone: + 31(0)222369416
Fax: + 31(0)222319674

de Baar, Hein: NIOZ; Hein.de.Baar@nioz.nl
Royal Netherlands Institute for Sea Research
P.O. Box 59 1790 AB Den Burg The Netherlands
Phone: + 31 222 369465, Fax: + 31 222 319674
University of Groningen
Department Ocean Ecosystems
P.O. Box 14, 9750 AA Haren (Groningen)
Phone secretariat: + 31 50 363 2259

van den Berg, Stan: vandenberg@liverpool.ac.uk
University of Liverpool
Department of Oceans and Ecosystems
PO Box 147
Liverpool, United Kingdom
Phone: +44 151 794 4096

Boye, Marie: Marie.Boye@univ-brest.fr
Laboratoire des Sciences de l'Environnement Marin (LEMAR), CNRS-UMR 6539 Institut Universitaire Europaen de la Mer (IUEM)
Technopole Brest-Iroise
Place Nicolas Copernic
29280 Plouzané, FRANCE
Phone: 33 2 98 49 86 51 - Fax : 33 2 98 49 86 45

Clargo, Nikki: NIOZ; E-mail: Nikki.clargo@nioz.nl

Dulaquais, Gabriel: LEMAR IUEM; E-mail: Gabriel.Dulaquais@univ-brest.fr

Gerringa, Loes J.A., NIOZ; Loes.Gerringa@nioz.nl
Royal Netherlands Institute for Sea Research
BIO-Chemical Oceanography
PO Box 59 1790 AB Den Burg
The Netherlands
Phone: + 31(0)222369436
Fax: + 31(0)222319674

van Heuven, Steven: svheuven@gmail.com
Centrum voor Isotopen Onderzoek (CIO)
Energy and Sustainability Research Institute Groningen (ESRIG) Rijksuniversiteit Groningen
Nijenborgh 4, 9747 AG Groningen, Netherlands
Phone: +31-50-3634760
Fax: +31-50-3634738

Laan, Patrick: NIOZ; email: Patrick.Laan@nioz.nl

Maas, Leo: Leo.Maas@nioz.nl
Royal Netherlands Institute for Sea Research
Physical Oceanography
PO Box 59 1790 AB Den Burg
The Netherlands
Phone: + 31(0)222369419
Fax: + 31(0)222319674

van Mastrigt, Audrey: RuG; audrey@vanmastrigt.net
(See Willem van de Poll)

Meijer, Harro: h.a.j.meijer@rug.nl
Centrum voor Isotopen Onderzoek (CIO)
Energy and Sustainability Research Institute Groningen (ESRIG) Rijksuniversiteit Groningen
Nijenborgh 4, 9747 AG Groningen, Netherlands
Phone: +31-50-3634760
Fax: +31-50-3634738

Middag, Rob: NIOZ; email: rmiddag@chemistry.otago.ac.nz
Present address:
Department of Chemistry, University of Otago, Dunedin, New Zealand

Ober, Sven: NIOZ; Sven.Ober@nioz.nl

van de Poll, Willem: W.H.van.de.Poll@rug.nl
University of Groningen
Department of Ocean Ecosystems
Nijenborgh 7
9747 AG Groningen
The Netherlands
Phone: +31 50 363 7856

Rijkenberg, Micha: NIOZ, email: micha.rijkenberg@nioz.nl
Royal Netherlands Institute for Sea Research
P.O. Box 59 1790 AB Den Burg The Netherlands
Phone: 0031 222 369464
Fax: 0031 222 319674

Salaun, Pascal: pascal.salaun@liverpool.ac.uk
University of Liverpool
Department of Oceans and Ecosystems
PO Box 147
Liverpool, United Kingdom
Phone: +44 151 794 4101

de Steur, Laura: Laura.de.Steur@nioz.nl
Royal Netherlands Institute for Sea Research
P.O. Box 59 1790 AB Den Burg The Netherlands
Phone: 0031 222 369411
Fax: 0031 222 319674

Underwood, Jack: University of Utrecht; j_s_underwood@yahoo.co.uk
(See Leo Maas)

Vergouwen, Sophie: RuG; sophievergouwen@hotmail.com
(See Willem van de Poll)

Wuis, Leon: NIOZ; Leon.Wuis@nioz.nl

Appendix 2. Station list & devices deployment

UCC is the ultra clean CTD
Mooring is the LOCO2 mooring

Station	Cast	Device	Action	date & time	Latitude	Longitude
1	1	UCC	Begin	31/07/2012 10:51	60.663665	-34.936652
1	1	UCC	Bottom	31/07/2012 10:55	60.664108	-34.936359
1	1	UCC	End	31/07/2012 11:44	60.635458	-35.045117
2	1	mooring	Recovery	01/08/2012 09:04	59.204082	-39.500545
2	2	UCC	Begin	01/08/2012 14:30	59.206176	-39.507008
2	2	UCC	End	01/08/2012 15:02	59.205662	-39.507427
2	3	UCC	Begin	01/08/2012 16:35	59.206083	-39.508233
2	3	UCC	Bottom	01/08/2012 17:39	59.204771	-39.508772
2	3	UCC	End	01/08/2012 18:37	59.205429	-39.508653
2	4	mooring	Deployment	02/08/2012 16:29	59.201906	-39.504476
2	5	UCC	Begin	02/08/2012 17:22	59.189164	-39.513037
2	5	UCC	Bottom	02/08/2012 18:19	59.18936	-39.512945
2	5	UCC	End	02/08/2012 19:22	59.189121	-39.512675
3	1	UCC	Begin	03/08/2012 10:23	57.210872	-41.598975
3	1	UCC	Bottom	03/08/2012 11:30	57.211044	-41.599727
3	1	UCC	End	03/08/2012 13:47	57.211633	-41.598667
3	2	UCC	Begin	03/08/2012 16:15	57.211058	-41.599292
3	2	UCC	Bottom	03/08/2012 16:27	57.210932	-41.599185
3	2	UCC	End	03/08/2012 17:33	57.210722	-41.599122
4	1	UCC	Begin	04/08/2012 05:38	55.726744	-43.56289
4	1	UCC	Bottom	04/08/2012 06:41	55.726905	-43.563141
4	1	UCC	End	04/08/2012 08:48	55.72739	-43.561676
4	2	UCC	Begin	04/08/2012 11:36	55.72646	-43.562512
4	2	UCC	Bottom	04/08/2012 11:55	55.72669	-43.562705
4	2	UCC	End	04/08/2012 13:08	55.726644	-43.563054
5	1	UCC	Begin	05/08/2012 20:20	50.787578	-44.079288
5	1	UCC	Bottom	05/08/2012 21:43	50.789473	-44.06165
5	1	UCC	End	06/08/2012 00:03	50.798324	-44.024827
5	2	UCC	Begin	06/08/2012 03:01	50.788028	-44.075897
5	2	UCC	Bottom	06/08/2012 03:30	50.787572	-44.057697
5	2	UCC	End	06/08/2012 04:09	50.787007	-44.028388
6	1	UCC	Begin	08/08/2012 05:17	43.041122	-44.389654
6	1	UCC	Bottom	08/08/2012 06:42	43.041423	-44.389385
6	1	UCC	End	08/08/2012 09:15	43.041262	-44.389589
6	2	UCC	Begin	08/08/2012 12:14	43.04125	-44.389633
6	2	UCC	Bottom	08/08/2012 12:28	43.041377	-44.389335
6	2	UCC	End	08/08/2012 13:23	43.041296	-44.389615
7	1	UCC	Begin	09/08/2012 05:15	41.434346	-46.146667

7	1	UCC	Bottom	09/08/2012 06:44	41.434399	-46.146372
7	1	UCC	End	09/08/2012 09:17	41.434518	-46.147065
7	2	UCC	Begin	09/08/2012 11:11	41.43456	-46.146837
7	2	UCC	Bottom	09/08/2012 11:24	41.434481	-46.146635
7	2	UCC	End	09/08/2012 13:06	41.43438	-46.145487
8	1	UCC	Begin	10/08/2012 09:13	42.312407	-41.87929
8	1	UCC	Bottom	10/08/2012 09:26	42.309534	-41.879337
8	1	UCC	End	10/08/2012 10:21	42.297929	-41.881826
9	1	UCC	Begin	11/08/2012 09:09	43.34624	-36.807392
9	1	UCC	Bottom	11/08/2012 09:22	43.346028	-36.803065
9	1	UCC	End	11/08/2012 10:12	43.346862	-36.791747
10	1	UCC	Begin	12/08/2012 09:05	44.375288	-31.655383
10	1	UCC	Bottom	12/08/2012 09:19	44.374295	-31.655322
10	1	UCC	End	12/08/2012 10:08	44.372604	-31.6552
11	1	UCC	Begin	13/08/2012 09:05	45.409308	-26.419593
11	1	UCC	Bottom	13/08/2012 09:18	45.409538	-26.418763
11	1	UCC	End	13/08/2012 10:05	45.412126	-26.418296
12	1	UCC	Begin	14/08/2012 08:03	46.381463	-21.365696
12	1	UCC	Bottom	14/08/2012 08:15	46.381615	-21.364394
12	1	UCC	End	14/08/2012 08:59	46.38293	-21.365957
13	1	UCC	Begin	16/08/2012 07:30	48.431078	-10.417544
13	1	UCC	Bottom	16/08/2012 07:41	48.429525	-10.416307
13	1	UCC	End	16/08/2012 08:11	48.42685	-10.416312
14	1	UCC	Begin	17/08/2012 12:13	49.639453	-3.753096
14	1	UCC	Bottom	17/08/2012 12:23	49.638823	-3.759552
14	1	UCC	End	17/08/2012 12:41	49.637379	-3.769509